Title
Age-associated impairment of T cell immunity is linked to sex-dimorphic elevation of N-glycan branching.

Journal
Nature aging, 2(3)

ISSN
2662-8465

Authors
Mkhikian, Haik
Hayama, Ken L
Khachikyan, Khachik
et al.

Publication Date
2022-03-01

DOI
10.1038/s43587-022-00187-y

Peer reviewed

HHS Public Access

Author manuscript

Nat Aging. Author manuscript; available in PMC 2022 September 18.

Published in final edited form as:

Nat Aging. 2022 March ; 2(3): 231–242. doi:10.1038/s43587-022-00187-y.

Age-associated impairment of T cell immunity is linked to sex-dimorphic elevation of N-glycan branching

Haik Mkhikian[1,*], **Ken L. Hayama**[2,*], **Khachik Khachikyan**[3], **Carey Li**[3], **Raymond W. Zhou**[3], **Judy Pawling**[4], **Suzi Klaus**[2], **Phuong Q.N. Tran**[3], **Kim M. Ly**[3], **Andrew D. Gong**[3], **Hayk Saryan**[3], **Jasper L. Hai**[3], **David Grigoryan**[3], **Philip L. Lee**[3], **Barbara L. Newton**[3], **Manuela Raffatellu**[2,5,6], **James W. Dennis**[4,7], **Michael Demetriou**[2,3,$]

[1]Department of Pathology and Laboratory Medicine, University of California, Irvine, Irvine, CA, USA

[2]Department of Microbiology and Molecular Genetics, University of California, Irvine, Irvine, CA, USA

[3]Department of Neurology, University of California, Irvine, Irvine, CA, USA

[4]Lunenfeld-Tanenbaum Research Institute, Mount Sinai Hospital, Toronto, Ontario, Canada

[5]Division of Host-Microbe Systems and Therapeutics, Department of Pediatrics, University of California, San Diego, La Jolla, CA, USA

[6]Chiba University-UC San Diego Center for Mucosal Immunology, Allergy, and Vaccines, La Jolla, CA, USA

[7]Department of Molecular Genetics, University of Toronto, Toronto, Ontario, Canada

Abstract

Impaired T cell immunity with aging increases mortality from infectious disease. The branching of Asparagine-linked glycans is a critical negative regulator of T cell immunity. Here we show that branching increases with age in females more than males, in naïve more than memory T cells, and in $CD4^+$ more than $CD8^+$ T cells. Female sex hormones and thymic output of naïve T cells (T_N) decrease with age, however neither thymectomy nor ovariectomy altered branching. Interleukin-7 (IL-7) signaling was increased in old female more than male mouse T_N cells, and triggered increased branching. N-acetylglucosamine, a rate-limiting metabolite for branching, increased with age in humans and synergized with IL-7 to raise branching. Reversing elevated branching rejuvenated T cell function and reduced severity of *Salmonella* infection in old female mice. These

[$]Correspondence to: Michael Demetriou, Department of Neurology, University of California Irvine, 208 Sprague Hall, Irvine, CA 92697, USA; Phone: (949) 824-9775, mdemetri@uci.edu.

[*]These authors contributed equally to this work.

Author Contributions

Conceptualization, H.M. and M.D.; Methodology, K.L.H., H.M., S.K., M.R., J.P., J.W.D., and M.D.; Investigation, K.L.H., H.M., K.K., C.L., R.W.Z., J.P., S.K., P.Q.N.T, K.M.L., A.D.G., J.L.H., D.G., P.L.L., H.S., and B.L.N. Writing – Original Draft, K.L.H, H.M. and M.D.; Writing – Review and Editing, H.M. and M.D.; Visualization, K.L.H, H.M. and M.D.; Supervision, H.M., M.R., J.W.D., and M.D.; Funding Acquisition, M.R. and M.D.

Competing Interests Statement

JD and MD are named as inventors on a patent application that describes GlcNAc as a biomarker for multiple sclerosis. JD and MD are named as inventors on a patent for use of GlcNAc in MS. The remaining authors declare no competing interests.

data suggest sex-dimorphic antagonistic pleiotropy, where IL-7 initially benefits immunity through T_N maintenance but inhibits T_N function by raising branching synergistically with age-dependent increases in N-acetylglucosamine.

Keywords

Immunosenescence; T cell, infection; N-glycosylation; N-glycan branching; N-acetyglucosamine; interleukin-7; aging; immunity

Aging associated immune dysfunction, referred to as immunosenescence, contributes to increased morbidity and mortality from both infectious and neoplastic diseases in older adults (i.e. adults ≥65 years old) [1,2]. For example, ~89% of the annual deaths from influenza in the U.S. are in people ≥65 years old, despite this age group representing only ~15% of the U.S. population[3]. The vulnerability of older adults to viral infections has been tragically highlighted by the recent emergence of SARS-CoV-2[4]. Increased morbidity and mortality in this age group also occurs with common bacterial infections such as those caused by the enteric pathogen *Salmonella*[5]. Furthermore, efficacy of immunizations declines with age[6,7] further increasing risk of infection in older adults. The rapidly aging population in the developed world exacerbates this issue and heightens the need for interventions that effectively target immunosenescence.

A number of age associated changes in T cell numbers and functionality have been identified. The frequencies of naïve versus central and/or effector memory T cells change substantially with age in both mice and humans, as the accumulation of antigenic experience promotes conversion of naïve cells to memory cells. Naïve T (T_N) cell numbers are maintained by production of new T_N cells in the thymus and by interleukin-7 (IL-7) dependent homeostatic proliferation in the periphery[8]. In mice, although the thymus involutes with age, thymic production remains a major contributor of T_N cell production throughout much of adult life. In humans by contrast, thymic production decreases dramatically early in life and T_N cell numbers are maintained primarily through peripheral IL-7 dependent proliferation[9]. Despite these changes, the size of the $CD4^+$ T_N cell pool is largely maintained throughout life and the T-cell receptor (TCR) repertoire decreases only mildly[10]. T cell function is also altered with age, with $CD4^+$ T_N cells exhibiting diminished signaling and activation in response to TCR stimulation[11]. However, despite the identification of multiple contributing deficits in T cell dysfunction, the underlying molecular mechanisms remain incompletely understood.

Asn (N) – linked glycans play a critical role in controlling T and B cell immunity in mice and humans[12–22]. The ER/Golgi secretory pathway in animal cells modifies nearly all cell-surface and secreted proteins via addition of complex carbohydrates. As these glycoproteins transit through the secretory pathway, their N-glycans are further modified by a set of resident glycosylation enzymes. N-acetylglucosaminyltransferases I, II, III, IV, and V (encoded by *Mgat1*, *Mgat2*, *Mgat3*, *Mgat4a*/*b*, and *Mgat5*) initiate N-acetylglucosamine (GlcNAc) branches that are variably extended/modified with galactose, sialic acid, fucose and/or sulfate (Extended Data Fig. 1a). This remodeling regulates ligand production for multivalent animal lectins (e.g. galectins, siglecs, and C-type lectins). Our work has

revealed that galectins bind TCR and other glycoproteins at the cell surface, forming a molecular lattice that impacts clustering, signaling and endocytosis of surface receptors and transporters to affect cell growth, differentiation and disease states in mice and humans[12–21,23–26]. In T cells, N-glycan branching and the galectin lattice negatively regulate TCR clustering/signaling, promote surface retention of Cytotoxic T-Lymphocyte Antigen 4 (CTLA-4), inhibit inflammatory T_H1 and T_H17 while promoting anti-inflammatory T_H2 and induced T regulatory cell (iTreg) differentiation and suppress development of autoimmunity in mice and humans[12–18,20,27,28].

The degree of N-glycan branching is among the main determinants of galectin lattice strength. Branching in turn is regulated by a complex network of genetic, metabolic and environmental factors that converge on the N-glycan branching pathway. These include multiple disease-associated polymorphisms, dietary intake of glycan building blocks, and metabolic production of uridine diphosphate N-acetylglucosamine (UDP-GlcNAc), the common sugar nucleotide substrate of the branching enzymes. UDP-GlcNAc is produced either by *de novo* synthesis from glucose via the hexosamine pathway or by salvage of GlcNAc. *In vitro* and *in vivo* supplementation with GlcNAc enhances N-glycan branching in T cells and suppresses autoimmunity[16,17,29].

Given the importance of N-glycans in regulating T cell function, we investigated whether N-glycan branching is altered with age. Indeed, we discovered that aging in female > male mice and humans is associated with increases in branched N-glycans in T_N cells and that reversing this phenotype rejuvenates T cell responses. We further uncover that this sex-dimorphic trait arises from excessive IL-7 signaling in mice and synergy with age-dependent increases in serum GlcNAc in humans, identifying novel therapeutic targets for immunosenescence.

Results

N-glycan branching increases with age in female > male mouse T cells

To explore whether N-glycan branching increases with age, we compared L-PHA binding (*Phaseolus vulgaris, leukoagglutinin*) in splenic mouse T cells from old (74–113 weeks) and young (7–32 weeks) adult mice. L-PHA binds to β1,6GlcNAc-branched N-glycans (Extended Data Fig. 1a) and serves as a highly sensitive and quantitative marker of branching[14,30]. Flow cytometry revealed significant increases in branching in female splenic $CD4^+$ T cells, with differences in naïve (T_N) > central memory (T_{CM}) > effector memory (T_{EM}) cells (Fig. 1a–c and Extended Data Fig. 1b,c). Consistent with elevated branching, high-mannose structures as measured by *conconavalin A* (ConA) binding were reduced in old female $CD4^+$ T_N cells (Extended Data Fig. 1a,d). Female $CD4^+$ T_N cells from peripheral lymph nodes were similarly elevated (Extended Data Fig. 1e). As only a ~20% change in branching is sufficient to alter T cell function and inflammatory disease risk[29,30], the observed increases are biologically significant. Importantly, the L-PHA binding of both young and old female T_N cells follows a similar Gaussian distribution, demonstrating that branching is elevated in the entire population and not due to unaccounted for heterogeneity within the $CD4^+$ T_N cell gate (Fig. 1b). In contrast, L-PHA histograms of the memory populations demonstrated broader multi-modal peaks which shifted toward higher average

mean fluorescence intensities (MFIs) but remain overlapping when comparing young and old. This suggests that unlike T_N cells, the smaller L-PHA binding increases in the memory populations may in part or completely be due to shifts in unaccounted subset frequencies.

Strikingly, although L-PHA binding in old male naïve and memory $CD4^+$ T cells was also elevated relative to young cells (Fig. 1d and Extended Data Fig. 1f), the effect was less consistent and of a markedly smaller magnitude than for old female $CD4^+$ T cells (e.g. a mean increase of 17.1% for male vs 70.2% for female $CD4^+$ T_N cells) (Fig. 1c,d and Extended Data Fig. 1g). Naïve but not memory female $CD8^+$ T cell also displayed elevated L-PHA binding relative to young cells (Fig. 1e), while male $CD8^+$ T cells again displayed smaller age-dependent differences (Fig. 1f). $CD19^+$ B cells in both males and females lacked notable differences in L-PHA binding with age (Extended Data Fig. 1h). T_N output from the thymus decreases significantly in old mice. Although N-glycan branching regulates T cell production from the thymus[27], single and double positive thymocytes exhibited no age-dependent differences in L-PHA binding (Extended Data Fig. 1i). This indicates that the increase in N-glycan branching in old T_N cells arises in the periphery rather than from alterations in thymocyte development in old mice. Together, these data show that N-glycan branching increases with age in female > male mouse T cells, with the greatest difference being in the $CD4^+$ T_N subset.

IL-7 signaling increases with age to raise N-glycan branching

To identify potential mechanisms driving elevated branching, we first sought to determine whether increased branching in old female T_N cells arises from cell-intrinsic and/or cell-extrinsic factors. To assess this, we normalized the environment of $CD4^+$ T cells from young and old female mice by culturing them in media for 3 days *in vitro*. Indeed, equalizing external factors significantly reduced the difference in N-glycan branching between young and old female $CD4^+$ T_N cells, albeit aged T cells still retained higher branching compared to young T cells (Fig. 2a). Similarly, adoptively transferring congenically marked old female $CD4^+$ T_N cells into young recipient female mice for two weeks also significantly reduced the difference in N-glycan branching between young and old $CD4^+$ T_N cells (Fig. 2b and Extended Data Fig. 2a). Thus, cell-extrinsic factors in old female mice primarily drive increases in N-glycan branching.

To further explore mechanism, we sought to leverage the striking sex difference of the age-associated elevation in branching. We reasoned that age-associated gene-expression changes enriched in female compared to male T cells, and T_N compared to T_{EM} cells were likely involved. We thus performed RNA-sequencing (RNA-seq) analysis on FACS sorted, highly purified young and old $CD4^+$ T_N and T_{EM} cells from female and male mice with representative changes in branching (Extended Data Fig. 2b,c). Principal component analysis revealed that $CD4^+$ T_N clustered tightly together regardless of age and sex (Extended Data Fig. 2c). Moreover, the T_N population was widely separated from the T_{EM} cell populations, indicating that the purified $CD4^+$ T_N cells are not significantly contaminated by memory cells. Comparing young and old $CD4^+$ T_N cells, 158 and 192 differentially expressed genes (DEGs) were identified in females and males, respectively. Remarkably, only 44 of these overlapped between the sexes (Extended Data Fig. 2d, Supplementary Tables 1–3). There

were no significant differences in gene expression of N-glycan branching enzymes or other relevant glycosylation genes (Supplementary Table 4), which we confirmed by qPCR for critical Golgi branching enzymes (Extended Data Fig. 2e).

Among the 114 DEGs in female but not male $CD4^+$ T_N cells, four were within the IL-7 signaling pathway (Table 1), a pathway previously implicated in regulating N-glycan branching [17]. This included reduced expression of interleukin-7 receptor alpha chain (*Il7r*) and increased expression of Suppressor of cytokine signaling 1 (*Socs1*), *Socs3*, and Janus kinase 3 (*Jak3*). Other IL-7 signaling pathway genes were unchanged (Table 1). Flow cytometry confirmed that IL7Rα protein was reduced in aged female > male $CD4^+$ T_N cells (Fig. 2c, Extended Data Fig. 2f) and correlated strongly with the magnitude of branching elevation (Extended Data Fig. 2g). In contrast, IL7Rα protein expression was unchanged in old male and female $CD4^+$ T_{EM} cells (Extended Data Fig. 2h,i). IL-7 signaling is known to downregulate IL7Rα levels, suggesting that the decrease observed may be secondary to excessive IL-7 signaling in old female T_N cells [8,31]. Indeed, IL7Rα levels and phosphorylation of the downstream signaling molecule STAT5 (pSTAT5) are proxy measures of IL-7 signaling [32]. Consistent with this hypothesis and the observed IL7Rα expression levels, old female $CD4^+$ T_N cells but not T_{EM} cells displayed increased basal pSTAT5 (Fig. 2d). Note that IL-7 has a short serum half-life in mice (~2 hrs) and was not detectable by ELISA in the serum of old female mice.

To directly examine whether increased IL-7 signaling enhances N-glycan branching, we cultured old and young resting $CD4^+$ T cells with recombinant IL-7. Indeed, IL-7 significantly increased N-glycan branching in both old and young, male and female $CD4^+$ T_N cells (Fig. 2e,f), with no differences noted between the sexes. To confirm that IL-7 signaling also increases N-glycan branching in $CD4^+$ T_N cells *in vivo*, we administered IL-7 as a complex with the anti-IL-7 monoclonal antibody M25 into young mice. As a pre-formed complex, IL-7/M25 improves IL-7 half-life and markedly increases biological activity *in vivo* [33]. The IL-7/M25 complex at two different doses significantly increased N-glycan branching levels in $CD4^+$ T_N cells of young mice *in vivo* (Fig. 2g). To confirm that excessive IL-7 signaling was increasing N-glycan branching in $CD4^+$ T_N cells of old female mice, we injected high doses of the anti-IL-7 M25 antibody, which blocks endogenous IL-7 signaling at these doses [34]. Indeed, two weeks of anti-IL-7 antibody (M25) treatment reduced N-glycan branching levels in old female $CD4^+$ T_N cells down to that of young cells in both blood and spleen (Fig. 2h,i). This treatment also appeared to partially reverse the reduction in IL7Rα protein expression present in old female $CD4^+$ T_N cells (Extended Data Fig. 2j). As two weeks of inhibiting IL-7 may be too short to fully reverse the down-regulation of IL7Rα, we repeated the anti-IL-7 antibody (M25) treatment for four weeks. In addition to lowering N-glycan branching (Extended Data Fig. 2k,l), the longer treatment reversed the reduction in IL7Rα protein expression as well as the elevation in basal pSTAT5 levels in old female $CD4^+$ T_N cells (Fig. 2j,k). These reversals confirm that excessive IL-7 signaling *in vivo* is responsible for reduced IL7Rα and elevated basal pSTAT5 in old female mice. More broadly, the combined data indicate that elevated IL-7 signaling in old female > male $CD4^+$ T_N cells raises N-glycan branching.

IL-7 is critical for homeostatic maintenance of T cells and may be increased co-incident with thymic involution as T cells rely more on homeostatic proliferation. Alternatively, with reduced thymic output, existing T_N cells may enjoy a greater share of available IL-7, leading to increased IL-7 signaling [35]. We thus sought to determine if thymectomy in young female mice could drive N-glycan branching by increasing IL-7 signaling in $CD4^+$ T_N cells. Although thymectomized mice demonstrated a precipitous drop in $CD4^+$ T_N cells, neither IL7Rα protein levels nor N-glycan branching were changed in $CD4^+$ T_N cells (Extended Data Fig. 3a–c). Alternatively, loss of estrogen in old female mice may be responsible for altered IL-7 signaling and may explain the sex-dimorphic increase in branching. Indeed, ovariectomy has been shown to increase IL-7 levels in bone marrow [36]. Ovariectomy of young female mice resulted in a small reduction in IL7Rα levels (~15%) on $CD4^+$ T_N cells at four weeks post-surgery (Extended Data Fig. 3d). However, N-glycan branching levels remained unchanged (Extended Data Fig. 3e). Furthermore, branching levels did not change for up to 18 weeks post-ovariectomy and IL7Rα levels on $CD4^+$ T_N cells remained only ~15% reduced when measured at 23 weeks post-ovariectomy (Extended Data Fig. 3f,g). As $CD4^+$ T_N cells from old female mice demonstrated a ~50% reduction in IL7Rα levels (Fig. 2c and Extended Data Fig. 2g), the ~15% decrease in IL7Rα induced by ovariectomy appears insufficient to alter branching. To test whether the combined loss of estrogen and thymic output may be required, we examined mice that were both thymectomized and ovariectomized. Similar to ovariectomy alone, these mice demonstrated a small (15%) decrease in IL7Rα levels on $CD4^+$ T_N cells but no change in branching (Extended Data Fig. 3h,i). These data demonstrate that ovariectomy and thymectomy of young female mice in isolation or in combination is insufficient to drive increases in N-glycan branching on $CD4^+$ T_N cells. In summary, the IL-7 driven enhancement of N-glycan branching in T_N cells of old female mice appears largely independent of age-associated thymic involution and/or complete loss of ovarian function.

Elevated N-glycan branching in old T cells suppresses function

Age-dependent increases in N-glycan branching are expected to limit TCR induced activation and pro-inflammatory responses in old T cells[12–14,16–18]. To initially assess this, we compared induction of the T cell activation marker CD69 in response to anti-CD3 stimulation. Indeed, $CD4^+$ T cells from aged female mice were hypo-reactive in comparison to young $CD4^+$ T cells (Fig. 3a). This effect was reversed by treating T cells with the mannosidase I inhibitor kifunensine (KIF), which blocks N-glycan branching[18] (Fig. 3a). To confirm this using a genetic model, we examined aged mice with T cell specific deficiency of the Mgat2 branching enzyme (i.e. *Mgat2*$^{fl/fl}$*lck-cre* mice). T cells lacking *Mgat2* have reduced N-glycan branching and display hybrid N-glycans with a single branch extended by poly N-acetyllactosamine[18] (Extended Data Fig. 4a). Indeed, old *Mgat2* deficient $CD4^+$ T cells displayed enhanced induction of CD69 (Fig. 3b). Consistent with this data, T cell proliferation in old female $CD4^+$ T cells was also rejuvenated by decreasing branching with KIF or *Mgat2* deficiency (Fig. 3c). To confirm that reversing the increase in branching improves TCR signaling specifically in $CD4^+$ T_N cells, we examined the proximal TCR signaling pathway by phospho-flow cytometry of anti-CD3 antibody stimulated splenocytes and gating on the $CD4^+$ T_N pool. Dose-dependent increases in phosphorylation of ERK1/2, Zap70 and CD3-zeta were all significantly attenuated in old relative to young female $CD4^+$

T_N cells (Fig. 3d–f). However, modestly reducing branching in old female $CD4^+$ T_N cells by ~20%, via a 24hr pre-incubation with KIF (Extended Data Fig. 4b), readily rejuvenated the activation of ERK1/2, Zap70 and CD3-zeta in old female $CD4^+$ T_N cells (Fig. 3d–f). Moreover, phospho-ERK1/2 induction was also significantly increased by *Mgat2* deficiency in $CD4^+$ T_N cells (Extended Data Fig. 4c). Together, these data demonstrate that age-dependent elevation in branching functions to reduce TCR signaling thresholds in old $CD4^+$ T_N cells.

N-glycan branching also suppresses inflammatory T cell responses by both inhibiting pro-inflammatory T_H17 while promoting anti-inflammatory Treg differentiation[12,37]. Thus, age-dependent increases in N-glycan branching are expected to reduce T cell inflammatory responses in old adults. Indeed, blocking age-associated increases in N-glycan branching in old female $CD4^+$ T cells with either KIF or *Mgat2* deletion enhanced T_H17 differentiation while decreasing Treg induction (Extended Data Fig. 4d,e). Together, these results indicate that aging-induced increases in N-glycan branching functionally suppress pro-inflammatory T cell activity.

Elevated N-glycan branching suppresses immunity in old mice

In immune-competent hosts, non-typhoidal *Salmonella* (NTS) infection induces a robust T_H17 response and a localized self-limited infection within the gut mucosa [38,39]. However in old adults, NTS infection is a frequent cause of bacteremia [40], as the pathogen disseminates from the gut to systemic sites, a process that can be recapitulated in the mouse [41]. Prior studies have shown that T_H17 responses are critical to limit NTS dissemination from the gut [42,43]. Therefore, we sought to investigate whether the age-associated increases in N-glycan branching suppress T cell function *in vivo*, by employing an infectious colitis model with one of the most prevalent NTS serovar, *Salmonella enterica* serovar Typhimurium (*S.* Typhimurium). We infected old wild type female mice with a virulent strain of *S.* Typhimurium after streptomycin pre-treatment, as previously described [42]. This resulted in two deaths and high levels of *S.* Typhimurium recovered from the Peyer's patches, the mesenteric lymph nodes and the spleen, consistent with the pathogen's dissemination from the gut to systemic sites (Fig. 4a–c). In contrast, infecting age-matched T cell specific *Mgat2* deficient female mice in parallel (i.e. $Mgat2^{fl/fl}$*lck-cre*) resulted in no deaths and reduced colonization of Peyer's patches, mesenteric lymph nodes, and the spleen (Fig. 4a–c). *S.* Typhimurium colonization of the cecal content did not differ between control and *Mgat2* deficient old female mice (Extended Data Fig. 4f). Infected *Mgat2* deficient old female mice also displayed increased IL-17^+ and reduced $FoxP3^+$ cells within the bowel compared to infected controls (Fig. 4d,e), consistent with our *in vitro* data that age-dependent increases in N-glycan branching suppresses T_H17 and enhances Treg responses. Collectively, these data indicate that age-dependent increases in N-glycan branching in female T cells promotes *S.* Typhimurium dissemination.

N-glycan branching is elevated in old human female T cells

To investigate whether N-glycan branching is similarly elevated with aging in humans, we examined females and males ranging in age from 19 to 98 years old. Humans displayed a similar phenotype as mice with age-dependent increases of N-glycan branching in $CD4^+$

T cells > $CD8^+$ T cells > B cells, females > males, and naïve > memory T cells (Fig. 5a–e and Extended Data Fig. 5a–d). Branching in $CD45RA^+CD45RO^-$ $CD4^+$ T_N cells demonstrated a Gaussian shift of the entire population, indicating that subset heterogeneity is not responsible for the observed increase (Fig. 5a). Restricting analysis to ages from 19 – 65 showed similar results in female $CD4^+$ T cells, demonstrating the data is not significantly skewed by those over 90 years old (Extended Data Fig. 5e,f). As with mice, we examined whether cell-intrinsic and/or cell-extrinsic factors were driving the age-associated increase in N-glycan branching. Indeed, normalizing cell-extrinsic factors by resting peripheral blood mononuclear cells (PBMCs) in culture for four days resulted in a significant decrease in age-associated differences in branching in $CD4^+$ T_N cells (Extended Data Fig. 5g).

IL-7 and GlcNAc synergistically raise branching in old human T_n cells

As in mice, IL-7 signaling also downregulates IL7Rα expression in human T cells [44,45]. Furthermore, IL7Rα levels have been reported to decrease in human T_N cells with age, suggesting that IL-7 signaling increases with age [46,47]. We previously reported that short-term *in vitro* treatment of resting human $CD4^+$ T cells (mixed naïve and memory) for three days with IL-7 lowers branching[17], which is opposite to effects on mouse $CD4^+$ T_N cells described above. However, this analysis was agnostic to gender and naïve vs memory cells. We repeated these experiments but specifically analyzed resting female $CD4^+$ T_N and $CD8^+$ T_N cells and increased exposure to IL-7 to nine days, the latter to better reflect long term exposure *in vivo*. This revealed that exogenous IL-7 induced a small but statistically significant increase in N-glycan branching in T_{EM} cells, but was insufficient to increase branching in naïve T cells (Fig. 6a,b and Extended Data Fig. 6a,b).

IL-7 regulates mRNA expression of *Mgat1* in human T cells, where increased activity can either raise or lower branching depending on metabolic supply of UDP-GlcNAc substrate to the Golgi branching enzymes[17]. The Mgat1, 2, 4 and 5 branching enzymes all utilize UDP-GlcNAc as a donor substrate, but with declining efficiency (Extended Data Fig. 1a). The Km of Mgat4 and 5 for UDP-GlcNAc is ~100–200 fold worse than Mgat1 (~0.04 mM). Thus, when UDP-GlcNAc is limiting, elevated Mgat1 activity paradoxically lowers branching by outcompeting Mgat4 and 5 for their common substrate. However, with higher UDP-GlcNAc levels, Mgat5 activity is not limited and increased Mgat1 expression enhances branching, as would be expected[17]. This suggests that in humans, IL-7 induced increases in Mgat1 activity may synergize with an age dependent increase in UDP-GlcNAc.

UDP-GlcNAc biosynthesis by the hexosamine pathway is inhibited metabolically by aerobic glycolysis and glutaminolysis via inhibition of *de novo* synthesis from glucose but increased by salvage of N-acetylglucosamine (GlcNAc)[12,16,29]. Supplementing cells, mice or humans with GlcNAc increases UDP-GlcNAc levels and N-glycan branching in activated > resting T cells[12,16,17,24,29]. Interestingly, using targeted liquid chromatography - tandem mass-spectroscopy (LC-MS/MS) to assess GlcNAc and its stereoisomers (i.e. N-acetylhexosamines or HexNAc) in human serum revealed marked increases with age in both females and males (Fig. 6c,d)[48,49]. However, endogenous serum HexNAc levels positively correlated with N-glycan branching in $CD4^+$ T_N cells of females but not males (Fig. 6e,f), paralleling the age dependent increase in N-glycan branching being greater in

females. In contrast, HexNAc levels in old female mice were not significantly elevated compared to young female mice (Extended Data Fig. 6c), consistent with the greater direct effect of IL-7 on branching in mouse $CD4^+$ T_N cells. Consistent with IL-7 raising Mgat1 levels, co-incubating resting human female PBMCs with GlcNAc plus IL-7 for 9 days synergistically increased N-glycan branching in $CD4^+$ T_N cells (Fig. 6a,b), while having only an additive effect in $CD4^+$ T_{EM} cells (Extended Data Fig. 6a,b). Together, these data suggest that in humans, elevated IL-7 signaling of T_N cells synergizes with age-dependent increases in serum GlcNAc to raise N-glycan branching in naïve > memory and female > male T cells.

As with mice, the age-dependent elevation in N-glycan branching also suppressed T cell activity as treating old human female PBMCs with KIF to inhibit branching rejuvenated ligand-induced T cell activation and proliferation (Extended Data Fig. 6d,e). Reduced pERK levels in response to TCR stimulation are among the few functional defects specifically attributed to old human $CD4^+$ T_N cells[2,11]. To confirm that reversing the increase in branching improves TCR signaling specifically in $CD4^+$ T_N cells, old female PBMCs were pretreated with or without KIF for 24 hours to establish a ~15% reduction in LPHA staining (Extended Data Fig. 6f,g). They were then stimulated with anti-CD3 for 15 minutes prior to analysis of pERK levels by flow cytometry, gating specifically on $CD4^+$ T_N cells. Despite the small reversal in branching levels, KIF treatment significantly increased intracellular pERK levels, demonstrating that the age-associated increase in N-glycan branching acts to limit human $CD4^+$ T_N cell function (Fig. 6g).

Discussion

Our data reveal that human aging-associated increases in serum GlcNAc synergize with elevated IL-7 signaling to upregulate N-glycan branching and thereby induce hypo-activity of female > male naïve T cells. Our data also suggests an example of antagonistic pleiotropy, where a trait that is beneficial early becomes harmful later in life. IL-7 signaling is a critical mediator of peripheral T cell proliferation and homeostatic maintenance, particularly following loss of thymic output of T_N cells in early adulthood[45]. However, our data suggests that in later life excess IL-7 signaling in females > males can synergistically combine with age-dependent increases in GlcNAc to limit T_N function via increased branching. Thus, elevated IL-7 signaling may be beneficial through most of human adulthood, but contribute to immunosenescence in old females > males secondary to rising GlcNAc. Consistent with this hypothesis, reduced IL7Rα expression, a marker of elevated IL-7 signaling in humans[44,45], correlates with healthy aging and reduced immune related disorders in middle-age, yet also with decreased survival among both the middle-age and nonagenarians[50].

Early reports of T cell hypo-reactivity in older adults used mixed populations. In analyses of distinct T cell subsets, functional defects have persisted in $CD4^+$ T_N cells but have been brought into question for other subsets [2,11]. Interestingly, this pattern parallels the magnitude of N-glycan branching observed in this study, with $CD4^+$ > $CD8^+$ and T_N > T_{EM}. As age induced increases in N-glycan branching are reversed by cell culture, *in vitro* studies lasting days will underestimate the true extent of functional impairment. In this regard, *in vivo* studies and short-term *in vitro* signaling assays are likely more accurate.

Elevated IL-7 signaling was observed in female > male $CD4^+$ T_N cells but not $CD4^+$ T_{EM} cells. Moreover, exogenous IL-7 similarly raised branching in both male and female $CD4^+$ T_N cells regardless of age. This indicates that rather than a wholescale increase in IL-7 availability, cell-extrinsic differences in IL-7 signaling specific to T_N cells in females > males primarily drives the age-dependent increase in branching. As ovariectomy in mice did not enhance branching, the sex difference appears to be driven by sex chromosomes rather than female sex hormones. However, as ovariectomy also blocks androgens and other factors secreted by post-menopausal ovaries[51], a role for other secreted factors cannot be excluded. As there are several immune specific genes on the X chromosome, an effect of sex chromosomes could arise through incomplete X-inactivation of a gene(s) that regulates branching and survival of T_N cells. Indeed, our RNAseq data identified several genes located on the X chromosome with altered gene expression in old female but not male $CD4^+$ T_N cells.

Though previous studies have examined transcriptome changes in highly purified aged T cell subsets[52], we analyzed T cell populations by age and sex. Among the relatively few DEG's identified between young versus old $CD4^+$ T_N cells, less than 30% of these overlapped between males and females, suggesting sex-specific differences in T_N cell aging. Male-female differences in immune function are well described, such as the increased risk of many autoimmune diseases in females[53] and sex differences in morbidity and mortality to SARS-CoV-2[5455]. However, these sex differences can be mitigated or reversed in older adults. For example, onset of the autoimmune disease relapsing-remitting multiple sclerosis typically occurs in young adults (mean onset of age ~30) with a 3:1 ratio of female to males, but is only 1.5:1 in those who develop disease ≥ 65[56]. Moreover, while immune responses to vaccination are consistently higher in females than males throughout childhood and adulthood, this trend is reversed in aged individuals for the pneumococcal and Td/Tdap vaccines[57]. Furthermore, although females demonstrate higher antibody responses to influenza vaccination throughout life and in old age, old males produce higher avidity antibodies than old females indicating reduced T cell help in old females[58]. These reversals are consistent with the sex-dimorphic increase in N-glycan branching in older adults and imply that effective interventions of immune senescence may require sex-specific strategies.

Our data provide several potential therapeutic targets in T cell aging. First, the N-glycan branching pathway has known pharmacological inhibitors that have undergone human testing[59]. Though chronic use of these agents may be toxic, short term treatment during acute infection or at the time of vaccination may have benefit with limited toxicity. Development of T cell targeted strategies or novel inhibitors with better toxicity profiles are also attractive pursuits. Second, although IL-7 agonists have been extensively explored, our data suggests that this will lead to impaired T_N cell function via increased branching. Rather, co-administration of an IL-7 agonist with N-glycan antagonists should promote maintenance of the T_N cell pool while also ensuring that they are functional. Finally, reversing the elevation in serum GlcNAc either by limiting production, promoting metabolism/excretion or selective depletion may be an effective means of reversing T cell aging alone or in combination with IL-7 targeting agents.

Methods

Mice

All mouse experiments utilized C57BL/6 mice. C57BL/6 *Mgat2*$^{f/f}$ and *Mgat2*$^{f/f}$Lck-Cre were bred in house by initially crossing *Mgat2*$^{f/f}$ (JAX #006892) and Lck-Cre (JAX #003802) mice and are previously described[27]. Young and aged wild-type C57BL/6 mice were obtained from the National Institute of Aging (NIA) colony maintained at Charles River Laboratories (Wilmington, MA, USA). *Cd45.1* (JAX #002014) C57BL/6 mice were obtained from JAX. C57BL/6 mice were ovariectomized, thymectomized, ovariectomized and thymectomized, or subject to sham surgery by JAX surgical services at 9 weeks of age. For all experiments, delivered animals were allowed to acclimate to our vivarium for at least one week prior to measurements or the start of experiments. Mice were housed at the University of California, Irvine in an environment-controlled, pathogen-free barrier facility on a 12-h/12-h light/dark cycle at a constant temperature and humidity, with food and water available ad libitum. Young mice were 7–32 weeks old, while old mice were 74–130 weeks old. Age and sex information for particular experiments is indicated in the figures and/or figure legends. To acquire mouse plasma, blood was collected in sterile tubes containing 0.1M EDTA as an anticoagulant. The Institutional Animal Care and Use Committee of the University of California, Irvine, approved all mouse experiments and protocols (protocol number AUP-19–157).

Human subjects

Male and females subjects with an age range of 19–98 years old were examined in this study. Age and sex for particular experiments are indicated in the figures and/or figure legends. Individuals with cancer, uncontrolled medical disease or any other inflammatory syndrome were excluded. Human whole blood was collected from healthy individuals through the Research Blood Donor Program serviced by the Institute for Clinical & Translational Science (ICTS) or through The 90+ Study at the University of California, Irvine. All procedures with human subjects were approved by the Institutional Review Board of the University of California, Irvine. All study participants gave written informed consent and were uncompensated.

T cell isolation and culture

For *ex vivo* and *in vitro* mouse experiments, erythrocytes were depleted from splenic or lymph node cell suspensions by incubation with red blood cell (RBC) lysis buffer followed by negative selection using EasySep™ Naïve CD4$^+$ T Cell Isolation Kit or EasySep™ CD4$^+$ T Cell Isolation Kit (STEMCELL Technologies) according to manufacturer's instructions and supplemented with or without 20μg/mL biotinylated Phaseolus Vulgaris Leucoagglutinin (L-PHA, Vector Labs) to deplete non-*Mgat2* deleted cells. Freshly harvested cells were cultured (2×10^5-5×10^6 cells) in RPMI-1640 (Thermo Fisher Scientific) supplemented with 10% heat inactivated fetal bovine serum (Sigma Aldrich), 2μM L-glutamine (Gibco), 100U/mL penicillin/streptomycin (Gibco), and 50μM β-mercaptoethanol (Gibco) as previously described[14,16,27]. Human peripheral blood mononuclear cells (PBMCs) isolated by density gradient centrifugation over Histopaque-1077 (Sigma-Aldrich) or Lymphoprep (StemCell Technologies) were stimulated with plate-bound anti-CD3

(OKT3, eBioscience) plus soluble anti-CD28 (CD28.2, eBioscience) in media as described above. PBMCs were pre-treated with or without 5–10μM kifunensine 24 hours prior to stimulation if indicated. For pharmacological treatments, cells were incubated with GlcNAc (40mM added daily, Wellesley Therapeutics), kifunensine (5–10μM, Glycosyn), recombinant human IL-7 (50ng/ml *in vitro*; 0.5ug-1.5ug *in vivo*, R&D Systems), and/or anti-mouse/human IL-7 antibody (clone M25; 5–15ug, BioXCell) as indicated [60]. T_H17 and iTreg induction were performed as previously described [12].

Flow Cytometry

Flow cytometry experiments were performed as previously described[14,27]. Depending on cell yields and number of experimental conditions, cell staining was performed in two to four replicates. Mouse antibodies for surface, intracellular and phospho-flow staining to CD69 (H1.2F3), IL17 (eBio17B7), CD4 (RM4–5), CD8α (53–6.7), CD19 (1D3), Foxp3 (Fjk-16s), CD44 (IM7), CD62L (MEL-14), CD3 (145–2C11 and 17A2), CD25 (PC61.5), IL7Rα (A7R34), Rat IgG2a kappa Isotype Control (eBR2a), phospho-STAT5 (SRBCZX), phospho-CD247 (3ZBR4S), phospho-Zap70 (n3kobu5), and Mouse IgG1 kappa Isotype Control (P3.6.2.8.1) were purchased from eBioscience/ThermoFisher Scientific. In addition, antibodies to phospho-ERK1/2 (MILAN8R), CD45RA (HI100), CD4 (RM4–5), CCR7 (4B12), CD25 (BC96) and CD19 (HIB19) were purchased for human cells. Antibodies to mouse CD45.1 (A20), CD45.2 (104), phospho-ERK1/2(4B11B69), and anti-human CD45RO (UCHL1) and CD8 (SK1) were purchased from BioLegend. All antibodies were used at manufacturer recommended dilutions for flow cytometry. DyLight 649 conjugated Streptavidin, fluorescein labeled ConA, and both fluorescein labeled and biotinylated L-PHA were purchased from Vector Labs. Proliferation was assessed by staining cells with CellTrace CFSE proliferation kit (Thermo Fisher Scientific). Flow cytometry experiments were performed with the BD FACSAria Fusion Sorter, LSR II, Invitrogen Attune NxT Flow Cytometer, or ACEA Novocyte Flow Cytometer and analyzed following appropriate compensation using FlowJo software. The gating strategy used is demonstrated for $CD4^+$ T_N cells (Extended Data Fig. 1b).

Anti-CD3 stimulation and phospho-flow cytometry

Tissue culture treated flat bottom 96-well plates were coated with the indicated concentrations of functional grade anti-CD3e (anti-mouse clone 145–2C11; anti-human clone OKT3) in 100μl of PBS per well and incubated at 37°C for 3 hours or 4°C overnight. The anti-CD3 solution was then aspirated and replaced with 150μl of cells in complete medium at 2×10^6 cells/ml for human PBMCs or 6×10^6 cells/ml for mouse splenocytes. Plates were then centrifuged at 250rcf for 2 minutes to bring cells in contact with the bottom of the wells and incubated in a tissue culture incubator for 15 minutes. Cells were fixed by directly adding 100μl per well of 4% PFA, then resuspended, transferred to round-bottom plates, and incubated at 37°C for 15 minutes. For human PBMCs, cells were then permeabilized by resuspending in 200μl of ice cold methanol, followed by sealing the plate and vigorously votexing. Cells were left in methanol overnight at 4 °C, prior to washing and staining in routine FACS buffer. For mouse splenocytes, cells were permeabilized with 200μl of intracellular staining permeabilization wash buffer (Biolegend, 421002) instead of methanol and stained using this buffer instead of routine FACS buffer. Data was collected

on an ACEA Novocyte Flow Cytometer or Invitrogen Attune NxT Flow Cytometer and analyzed following appropriate compensation using FlowJo software.

Mouse *Salmonella* experiments

Mice were pre-treated with streptomycin (0.1 ml of a 200 mg/ml solution in sterile water) intragastrically one day prior to mock-infection or inoculation with *Salmonella enterica* serovar Typhimurium strain IR715, a nalidixic acid-resistant derivative of ATCC 14028s (5×10^8 CFU/animal). At 72 hours after infection, mice were euthanized and the cecal content, Peyer's patches, mesenteric lymph nodes, and spleen were collected for enumerating bacterial CFU through serial 10-fold dilutions plated on agar plates. Additionally, intestinal cells were isolated from approximately one third of the cecum and the entire colon by first cutting the cylindrical tissue lengthwise and cleaning the tissue of fecal matter by vigorously shaking the tissue in cold wash buffer (HBSS, 15mM HEPES, 1% antibiotic/antimycotic [Ab/Am]). The intestinal segments were cut into 3–5mm pieces on ice and were placed into gentleMACS C tubes (Miltenyi Biotec) with 10mL of prewarmed (37°C) HBSS containing 10% FBS, 15mM HEPES, 5mM EDTA, and 1% Ab/Am and ran twice on a GentleMACS dissociator (Miltenyi Biotec) using program m_spleen_04, incubated in a shaking water bath for 10 minutes, then spun down at 720 x *g* for 2 minutes. The supernatant containing intraepithelial cells were removed and placed on ice. The remaining tissue with lamina propria cells was washed with 30mL ice-cold IMDM solution containing 10% FBS and 1% Ab/Am then re-suspended in a 10mL mixture of Liberase (20μg/mL) and Collagenase (1mg/mL) in pre-warmed IMDM solution shaken at 37°C for 45 minutes. The digested tissues were placed in C tubes and underwent program B and m_spleen_04 on the GentleMACS dissociator. Afterwards, both the supernatant containing intraepithelial cells and the digested tissue containing lamina propria cells were further purified via Percoll gradient 40% on 80%, strained through a 70μm cell strainer (BD Biosciences) and pooled in IMDM solution for analysis of bowel cells.

Mouse adoptive transfer and IL-7 experiments

Lymphocytes were prepared from pooled inguinal lymph nodes and splenocytes and purified for naïve $CD4^+$ T cells from CD45.2 C56BL/6 donor mice as described above then injected intravenously by tail vein in 200μl of phosphate-buffered saline (PBS) into CD45.1 congenic C57BL/6 recipient mice. For *in vivo* IL-7 treatment, mice were i.p. injected with either 200μl of PBS or rhIL-7/M25 cytokine/antibody complex (R&D Systems and BioXCell) every two days. Before injection, the cytokine/antibody complex were generated through co-incubation for 30 mins at room temperature. GlcNAc was administered orally by adding GlcNAc to their drinking water at 1mg/ml. Fresh GlcNAc was given daily for the duration of the experiment. For IL-7 blockade experiments, mice were injected i.p. with 1–1.5mg of Mouse IgG1 isotype control antibody (MOPC-21, BioXCell) or anti-mouse/human IL-7 (M25, BioXCell) in 200μl of PBS three times at 2 day intervals per week as indicated.

RNA extraction, library preparation, and sequencing

Cell suspensions were prepared from pooled lymph nodes (axillary, brachial, cervical, and inguinal) and splenocytes, and then purified for $CD4^+$ T cells through negative selection by EasySep™ $CD4^+$ T cell Isolation Kit (STEMCELL Technologies). Cell suspensions

were then stained and FACS-sorted for either naïve ($CD3^+CD4^+CD25^-CD62L^+CD44^-$) or effector memory ($CD3^+CD4^+CD25^-CD62L^-CD44^+$) populations by BD FACSAria Fusion Sorter. Three biological replicates each with representative levels of N-glycan branching were obtained for young female $CD4^+$ T_N, old female $CD4^+$ T_N, young male $CD4^+$ T_N, old male $CD4^+$ T_N, young female $CD4^+$ T_{EM}, old female $CD4^+$ T_{EM}, young male $CD4^+$ T_{EM}, and old male $CD4^+$ T_{EM}.

Total RNA were then isolated using RNeasy Plus Micro Kit (Qiagen) and analyzed for RNA integrity number (RIN) by Agilent Bioanalyzer 2100. RIN of all samples was determined to be ≥9.0. Subsequently, 125ng of total RNA was used for library prep through NEBNext Poly(A) mRNA Magnetic Isolation Module before using NEBNext Ultra II DNA Library Prep Kit for Illumina. Collected samples was cleaned with AMPure XP beads (Beckman Coulter) to make RNA into strand specific cDNA libraries with multiplexing barcodes from NEBNext Multiplex Oligos for Illumina (Index Primers Set 1 and 2). RNASeq libraries were then analyzed by qPCR (KAPA Biosystem), normalized to 2nM and pooled for multiplexing in equal volumes, then underwent paired-end 100-bp sequencing run on HiSeq 4000 (Illumina).

The quality of the sequencing was first assessed using fastQC tool (v0.11.2). Raw reads were then adapter and quality trimmed and filtered by a length of 20 bases using trimmomatic (v0.35). Trimmed reads were mapped to the mouse mm10 reference genome using a splice aware aligner Tophat2 (v2.1.0) and resulting BAM files were processed using samtools (v.1.3), and gene expression was quantified with featureCounts (subread v2.0.1, featureCounts v1.5.0-p3) as raw counts and cufflinks (v2.2.1) as FPKM values. Raw counts were normalized and differential analysis was done using R package DESeq2 (v1.22.2) with a FDR cut off of 0.05. The associated analytical scripts can be found using the following link: (https://github.com/ucightf/demetriou). MDS plot was generated using limma (v3.38.3).

LC-MS/MS analysis

Human serum samples for metabolomics analysis were prepared as described previously [48]. Metabolites from 50µl of serum were extracted by the addition of 200µl of ice-cold extraction solvent (40% acetonitrile, 40% methanol, and 20% water). Thereafter the samples were shaken at 4°C for 1 hour at 1400rpm in a Thermomixer R (Eppendorf) and then centrifuged at 4°C for 10 minutes at ~18,000 x g in an Eppendorf microcentrifuge. The supernatant was transferred to fresh tubes and evaporated in a Speedvac (Acid-Resistant CentriVap Vacuum Concentrators, Labconco). The dry-extract samples were stored at −80°C. The dry eluted metabolites were resuspended in 100ul of water containing internal standards D^7-Glucose at 0.2mg/mL and H-Tyrosine at 0.02mg/ml. Eluted metabolites were analyzed in negative mode at the optimal polarity in MRM mode on electrospray ionization (ESI) triple-quadrupole mass spectrometer (AB Sciex 4000Qtrap, Toronto, ON, Canada). Standard curves were prepared by adding increasing concentrations of GlcNAc or N-Acetyl-D-[UL-$^{13}C_6$]glucosamine (Omicron Biochemicals) to 50µl aliquot of control serum. Raw data were imported to MultiQuant software (AB Sciex, Version 2.1) for peak analysis and manual peak confirmation. The resulting data including area ratio is then exported to Excel.

Statistical analysis

All statistical tests are non-parametric tests, except for Extended Data Figure 5g, where the Shapiro-Wilk normality test was performed and passed. Data where multiple independent experiments were normalized and combined are analyzed by the Wilcoxon non-parametric paired test. Statistical analyses were calculated with Prism software (GraphPad). *P* values were calculated from two/one-tailed Wilcoxon or Mann-Whitney tests unless specified otherwise. Details of test performed are found in the figure legends. One-tailed tests were performed only when directionality was predicted a priori. No statistical methods were used to pre-determine sample sizes but sample sizes were based on our previous experience performing comparable experiments and were similar to those reported in previous publications[11,18]

Randomization, blinding and data exclusion

Mice and humans were randomly selected and assessed. Mouse littermates were randomly distributed into treatment groups for *in vivo* experiments. Human participants were randomly enrolled and allocated based on age and gender. As physical attributes of mice are the same, no blinding was performed for mouse experiments. Human subjects were not blinded as this was an observational study rather than a clinical trial. The individuals performing serum measurements were blinded to sex and age. Quantification by flow cytometry was performed in a uniform manner for all samples. For all flow cytometry data, non-viable cells and doublets were excluded. In flow cytometry experiments, individual replicates were excluded if fluidics errors such as bubbles or clogging were detected during sample collection and significantly altered scattering characteristics or event counts. In Figure 2h, one mouse in the “12w.o. Isotype” group died on day 8, likely due to mishandling/misinjection, and could not be included in the 2 week time point. In Fig. 4b, one data point in the *Mgat2*$^{fl/fl}$ group could not be included due to failed MLN dissection. Data from experiments where positive and/or negative controls failed were excluded.

Data availability

RNA-seq data has been deposited with the Gene Expression Omnibus under accession number GSE184496. The mouse 10mm reference genome was obtained from https://hgdownload.soe.ucsc.edu/downloads.html#mouse. Statistical source data is provided for all main and extended data figures in supplemental information. Additional data that support the findings within this article are available from the corresponding author upon reasonable request.

Code availability

The code for differential analysis of RNA-seq data using R package DESeq2 has been uploaded to a github repository and can be found at https://github.com/ucightf/demetriou.

Extended Data

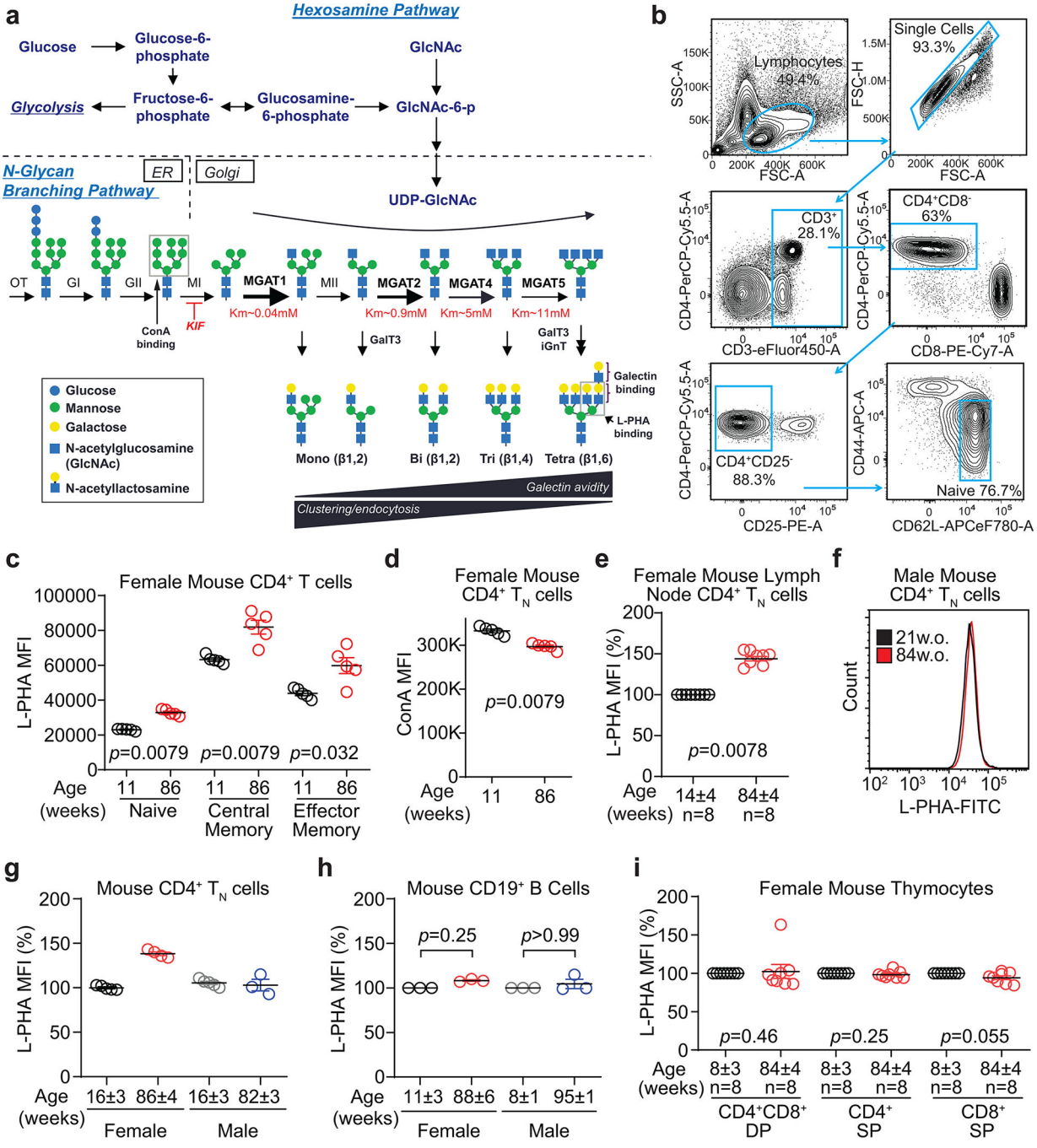

Extended Data Figure 1. Mouse T cells display a sex-dimorphic increase in N-glycan branching with age.

a) Fructose 6-phosphate may be metabolized by glycolysis or enter the hexosamine pathway to supply UDP-GlcNAc to the Golgi branching enzymes Mgat1, 2, 4 and 5, which generate mono-, bi-, tri-, and tetra-antennary GlcNAc branched glycans, respectively. The branching enzymes utilize UDP-GlcNAc with declining efficiency such that both Mgat4 and Mgat5 are limited for branching by the metabolic production of UDP-GlcNAc. Small molecule

inhibitor kifunensine (KIF) can be used to eliminate N-glycan branching. Plant lectin L-PHA (Phaseolus vulgaris, leukoagglutinin) binding sites are also shown. Abbreviations: OT, oligosaccharyltransferases; GI, glucosidase I; GII, glucosidase II; MI, mannosidase I; MII, mannosidase II; Mgat, N-acetylglucosaminyltransferase; GalT3, galactosyltransferase 3; iGnT, i-branching enzyme β1,3-N-acetylglucosaminyltransferase; KIF, kifunensine; GlcNAc, N-acetylglucosamine; UDP, uridine diphosphate; Km, Michaelis constant of the enzyme. **b)** The gating strategy is demonstrated for $CD4^+$ T_N cells. Lymphocytes were first gated on singlets, followed by gating on $CD3^+CD4^+CD8^-CD25^-CD62L^+CD44^-$ cells by sequential steps. **c, d)** Splenocytes from five young and old mice were analyzed for L-PHA (**c**) or ConA (**d**) binding by flow cytometry, gating on the indicated $CD4^+$ T cell subsets. Absolute geometric mean fluorescence intensity (MFI) is shown to allow direct comparison between naïve and memory subsets. **e-i)** $CD4^+$ T_N cells (**e-g**) $CD19^+$ B cells (**h**) or thymocytes (**i**) were obtained from the lymph node (**e**), spleen (**f-h**) or thymus (**i**) of female (**e, g-i**) or male (**f-h**) mice of the indicated ages, and analyzed for L-PHA binding by flow cytometry. Absolute or normalized geometric mean fluorescence intensity (MFI) are shown. Each symbol represents a single mouse. P-values by two-tailed Mann-Whitney (**c, d**) or two-tailed Wilcoxon (**e, h, i**). Error bars indicate mean ± s.e.m.

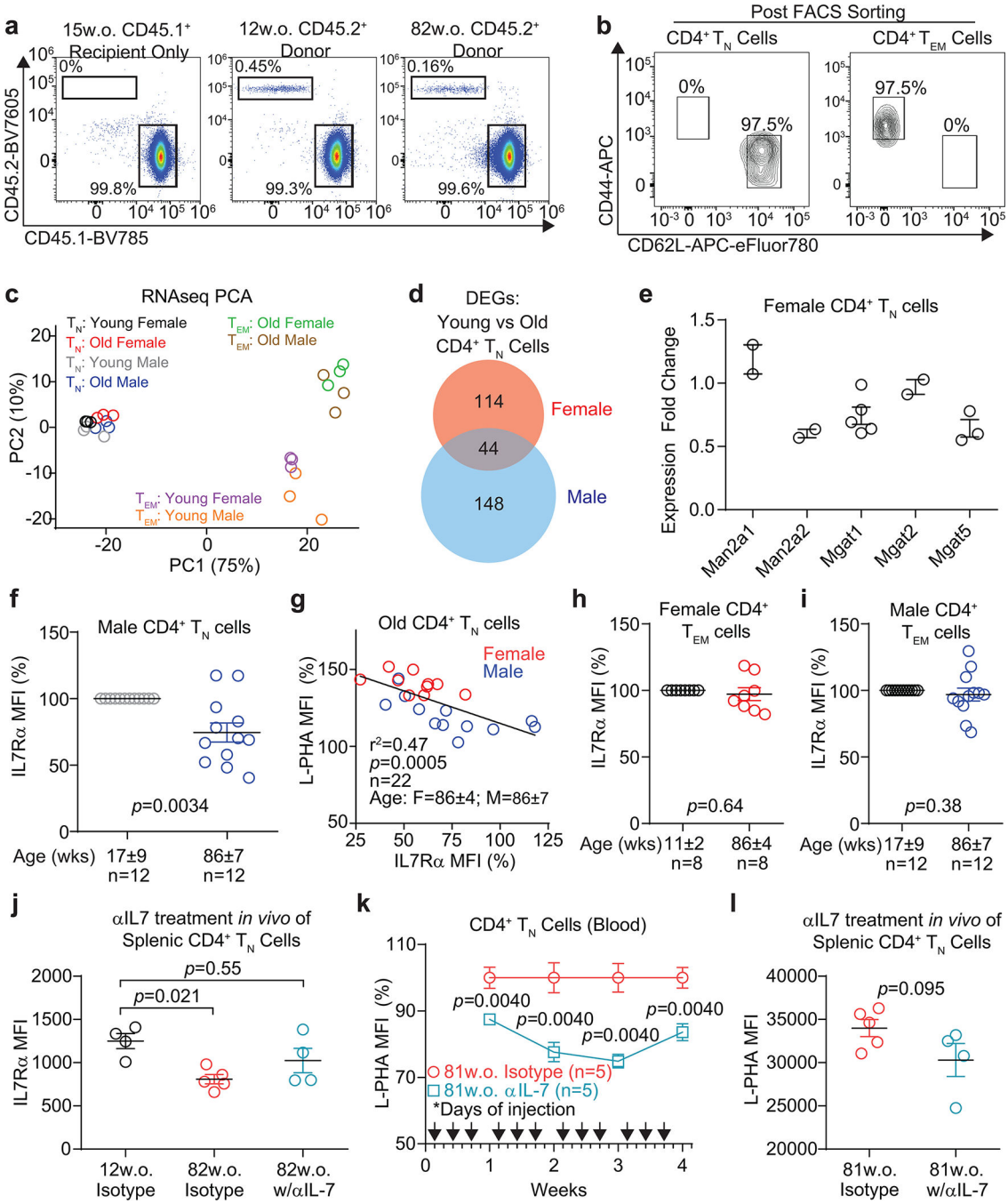

Extended Data Figure 2. Elevated IL-7 signaling increases N-glycan branching in old female naïve T cells.

a) Representative flow cytometry plots of donor and recipient cells post-adoptive transfer. **b)** Negatively selected $CD4^+$ T cells were FACS sorted for T_N ($CD62L^+CD44^-$) and T_{EM} ($CD62L^-CD44^+$) populations. Representative flow cytometry demonstrating purity of sorted cells used for RNA-seq. **c)** Principal component analysis (PCA) of RNA-seq data comparing gene expression in $CD4^+$ T_N and $CD4^+$ T_{EM} cells from young male (7–8 weeks old), young female (10–11 weeks old), old male (83–86 weeks old) and old female (85 weeks old) mice.

Three biological replicates were performed for each group. **d)** Out of 24062 genes analyzed by RNAseq, 158 DEGs were identified when comparing young and old $CD4^+$ T_N cells in females, 192 DEGs were identified in males, and 44 DEGs were shared. **e)** Young and old naïve $CD4^+$ T cell mRNA expression of N-glycan pathway genes by real-time qPCR. **f)** Flow cytometric analysis of IL7Rα in *ex vivo* $CD4^+$ T_N cells from young and old male mice. **g)** L-PHA versus IL7Rα expression in *ex vivo* $CD4^+$ T_N cells from old male and female mice. **h, i)** Flow cytometric analysis of IL7Rα in *ex vivo* young and old $CD4^+$ T_{EM} cells from female (**h**) and male (**i**) mice. **j-l)** C57BL/6 mice of the indicated ages were injected intraperitoneal with either isotype control (1.5mg) or anti-IL-7 antibody (M25, 1.5mg) three times per week for two (**j**) or four (**k, l**) weeks, and then analyzed for L-PHA or IL7Rα expression in blood (**k**) or spleen (**j, l**). Each symbol represents a single mouse unless specified otherwise. P-values determined by one-tailed Wilcoxon (**f**), linear regression (**g**), two-tailed Wilcoxon (**h, i**), Kruskal-Wallis with Dunn's multiple comparisons test (**j**), or one-tailed Mann-Whitney (**k, l**). Error bars indicate mean ± s.e.m.

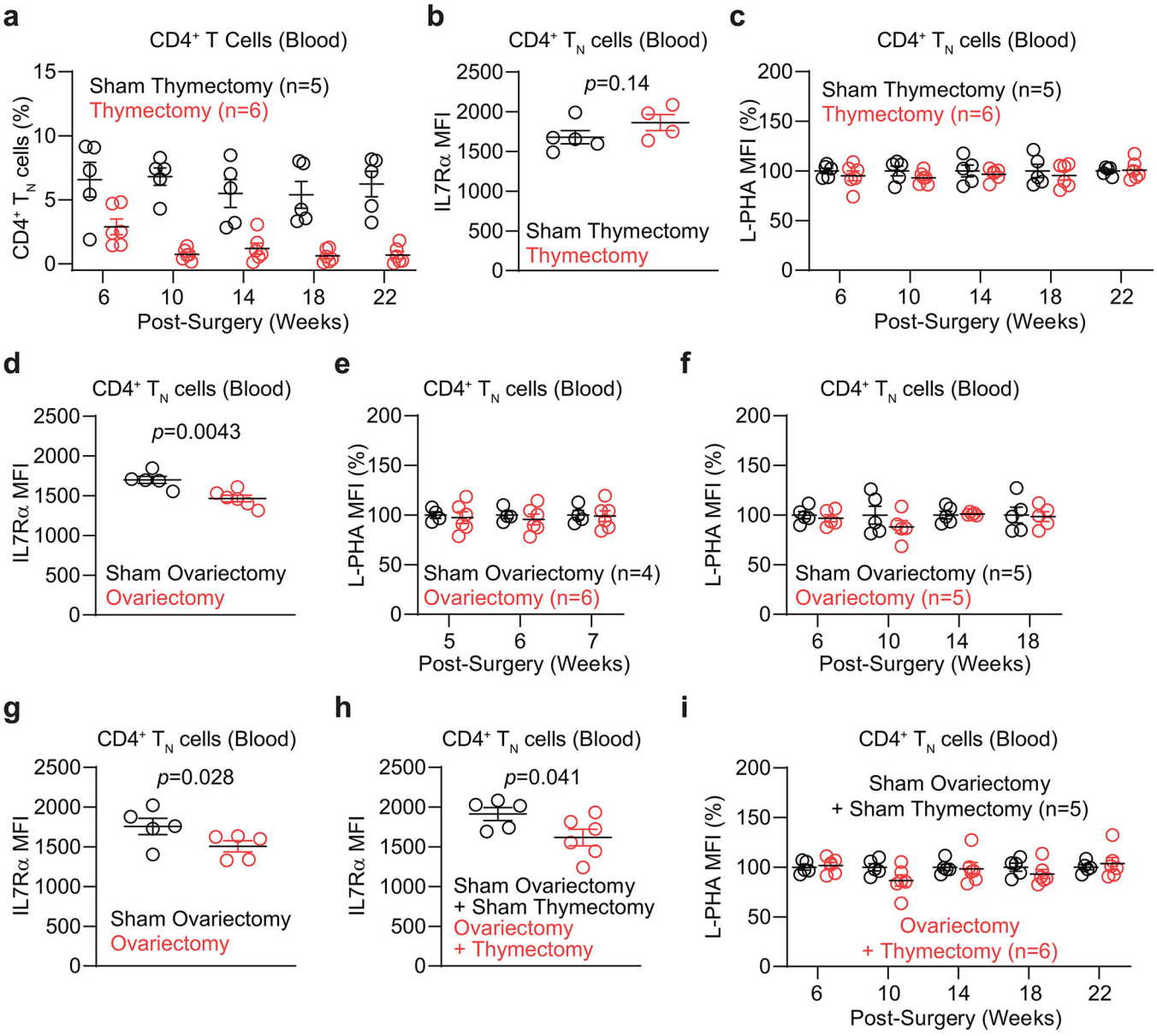

Extended Data Figure 3. Thymectomy and ovariectomy are insufficient to drive increases in N-glycan branching.

a-i) Female mice underwent thymectomy (**a-c**), ovariectomy (**d-g**), both surgeries (**h, i**), or corresponding sham procedures at the age of 9 weeks. Flow cytometry on blood at the indicated time points post-procedure was performed to detect percentage of $CD4^+$ T_N cells (**a**), IL7Rα expression (**b, d, g, h**), or L-PHA binding (**c, e, f, i**), gating on $CD4^+$ T_N cells. Absolute or normalized geometric mean fluorescence intensity (MFI) are shown. Each symbol at a particular time point represents a single mouse. P-values determined by one-tailed Mann-Whitney (**b, d, g, h**). Error bars indicate mean ± s.e.m

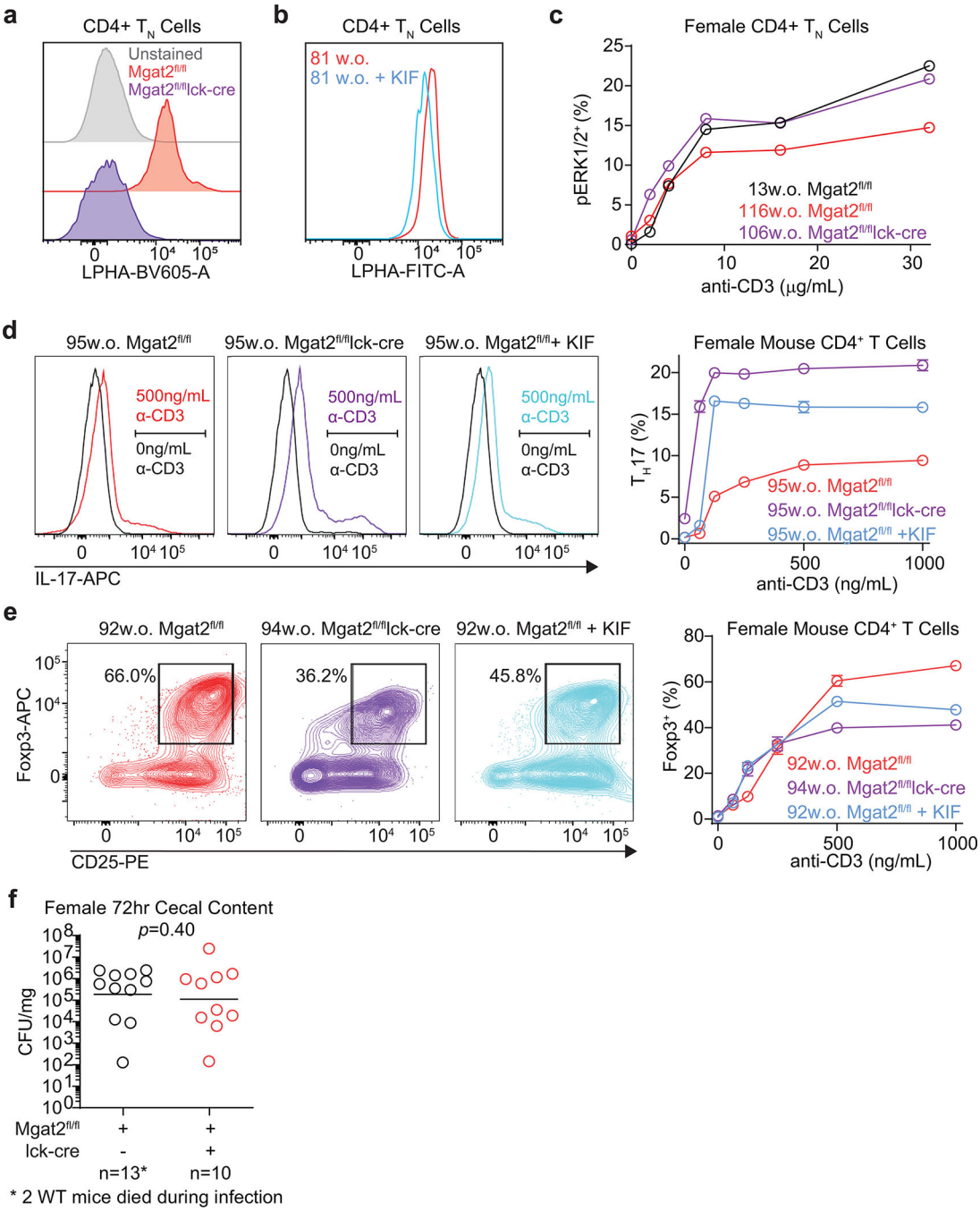

Extended Data Figure 4. Age-dependent increases in N-glycan branching suppress pro-inflammatory T cell function.

a) L-PHA binding of splenocytes from *Mgat2$^{fl/fl}$* and *Mgat2$^{fl/fl}$lck-cre* female mice, gated on CD4$^+$ T$_N$ cells. **b)** Splenocytes from an old mouse were treated with or without kifunensine for 24 hours, then analyzed for L-PHA binding by flow cytometry, gating on CD4$^+$ T$_N$ cells. **c)** Splenocytes from female mice of the indicated ages and genotypes were activated with plate bound anti-CD3 for 15 minutes. Following fixation and permeabilization, phospho-ERK1/2 induction was analyzed in CD4$^+$ T$_N$ cells by flow cytometry, gating additionally on

L-PHA negative cells in *Mgat2*$^{fl/fl}$*/lck-cre* mice. **d, e)** Flow cytometry analysis of purified mouse splenic CD4^{+} T cells activated with anti-CD3 and anti-CD28 for 4 days with T_H17 (TGFβ+IL-6+IL-23) or iTreg (TGFβ) inducing conditions, gating additionally on L-PHA negative cells in *Mgat2*$^{fl/fl}$*/lck-cre* mice. **f)** Female *Mgat2*$^{fl/fl}$ and *Mgat2*$^{fl/fl}$*lck-cre* mice were inoculated with streptomycin (0.1ml of a 200mg/ml solution in sterile water) intragastrically one day prior to inoculation with *S.* Typhimurium (5×10^8 colony forming units, CFU per mouse) by oral gavage. CFU in the cecal content was determined 72 hours after infection. Data shown are representative of two (**c**), or at least three (**a, b, d, e**) independent experiments. P-values by one-tailed Mann-Whitney (**f**). Error bars indicate mean ± s.e.m (**c, d, e**) or geometric mean (**f**).

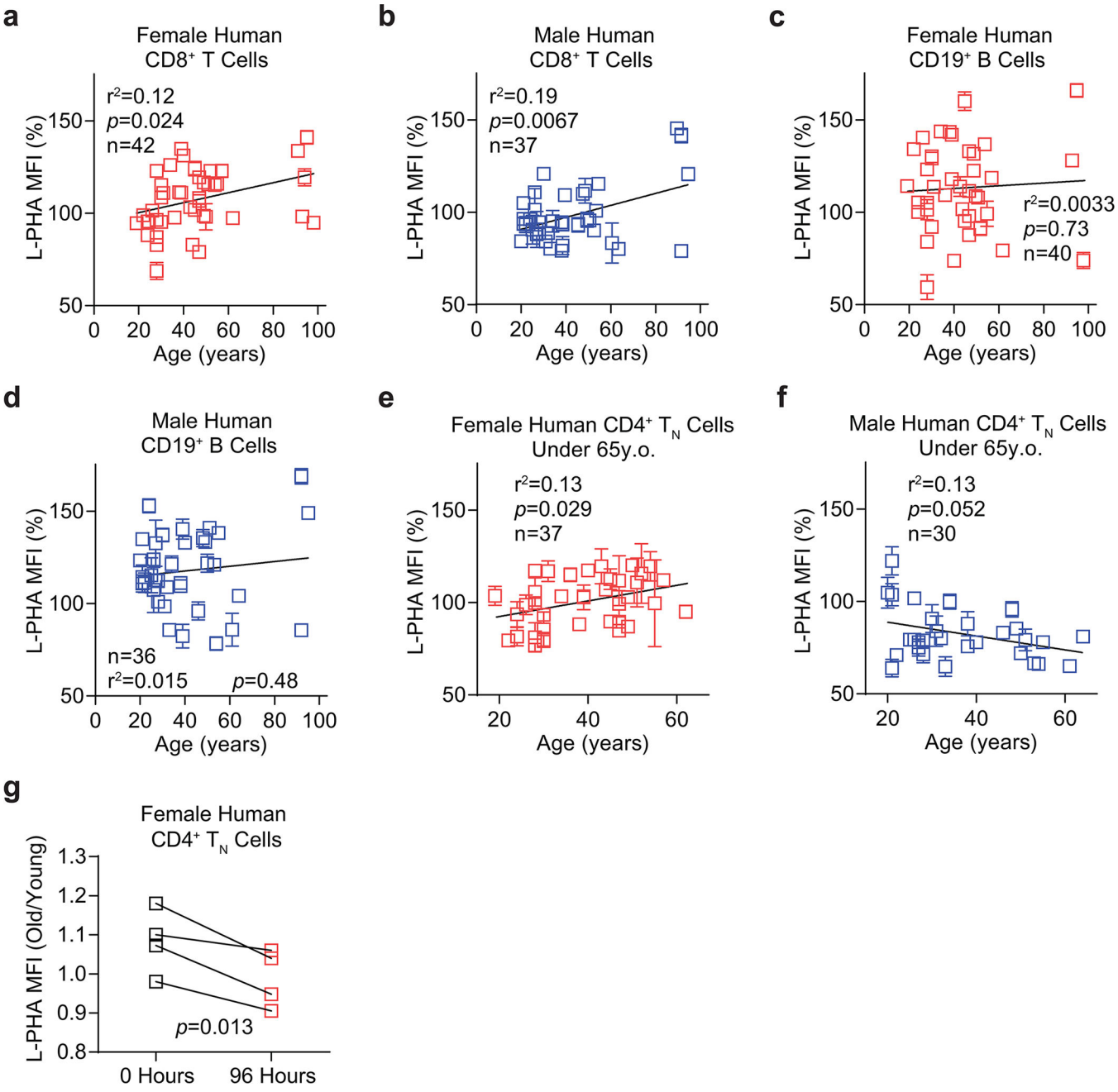

Extended Data Figure 5. Age-dependent increases in N-glycan branching suppress T cell activity in human females.

a-d) Human PBMCs from healthy females (**a, c**) or males (**b, d**) as indicated were analyzed for L-PHA binding by flow cytometry gating on $CD8^+$ T cells (**a, b**) or $CD19^+$ B cells (**c, d**). **e, f)** $CD4^+$ T_N cells ($CD45RA^+CD45RO^-$) from healthy females (**e**) and males (**f**) under the age of 65 were analyzed for L-PHA binding by flow cytometry. **g)** Human PBMCs from young (22–38 years old) and old (90–94 years old) female subjects were analyzed for L-PHA binding on $CD4^+$ T_N cells ($CD45RA^+CD45RO^-$) before or after 96 hours of culture in complete media. Shown is the ratio or each old subject over the average of the young at

the two timepoints. Each symbol represents a single individual. R^2 and p-values by linear regression (**a-f**) or by paired one-tailed t test, following passage of Shapiro-Wilk normality test (**g**). Error bars indicate mean ± s.e.m.

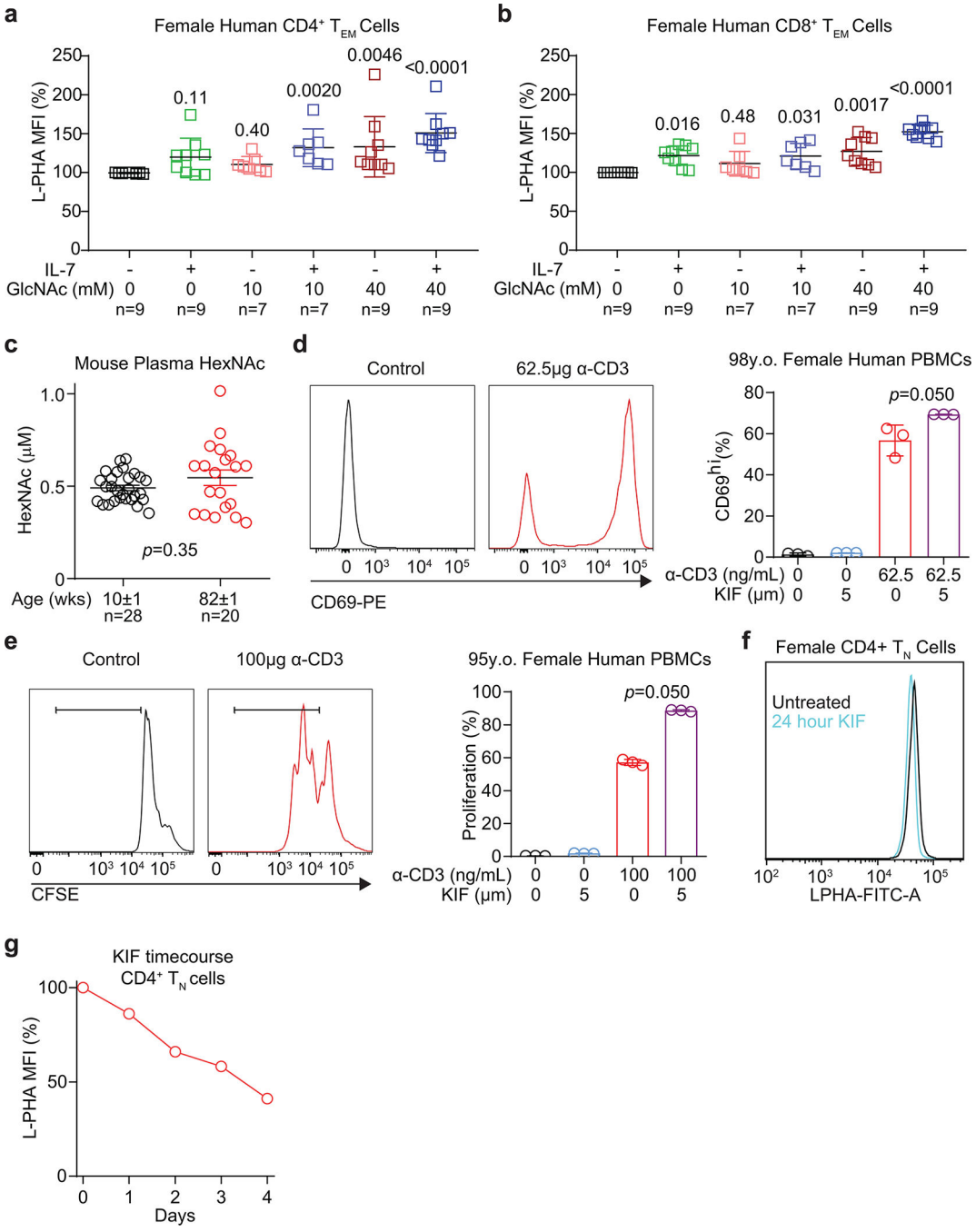

Extended Data Figure 6. N-acetylglucosamine and IL-7 synergize to raise N-glycan branching in human T cells.

a, b) PBMCs from nine healthy female donors (28–45 years old) were cultured with or without rhIL-7 (50ng/ml) and/or GlcNAc (10mM or 40mM) for 9 days, then analyzed for L-PHA binding by flow cytometry, gating on $CD4^+$ T_{EM} ($CD45RA^-CD45RO^+CCR7^-$) cells

(**a**) or $CD8^+$ T_{EM} ($CD45RA^-CD45RO^+CCR7^-$) cells (**b**). **c)** Mouse plasma from female mice of the indicated ages was analyzed for HexNAc levels by LC-MS/MS. **d, e)** Flow cytometric analysis of human PBMCs stimulated by anti-CD3 in the presence or absence of kifunensine as indicated for 24 hours to analyze for activation marker CD69 (**d**) or 72 hours to assess proliferation by CFSE dilution (**e**), gating on $CD4^+$ T cells. **f**) Female human PBMCs were treated *in vitro* with kifunensine for 24 hours, followed by analysis of L-PHA binding on $CD4^+$ T_N cells by flow cytometry. Data shown is representative of three independent experiments with different donors. **g**) Female human PBMCs were treated *in vitro* with kifunensine for up to four days, followed by analysis of L-PHA binding on $CD4^+$ T_N cells by flow cytometry. P-values by Kruskal-Wallis with Dunn's multiple comparisons test (**a, b**), two-tailed Mann-Whitney (**c**), and one-tailed Mann-Whitney (**d, e**). Error bars indicate mean ± s.e.m.

Supplementary Material

Refer to Web version on PubMed Central for supplementary material.

Acknowledgements

We thank Claudia Kawas (UC Irvine) for access to subjects from the "90+ cohort". Research was supported by the National Institute of Allergy and Infectious Disease (R01AI108917, M.D.; R01AI144403, M.D.; R01AI126277, M.R.; R01AI114625, M.R.), the National Center for Complementary and Integrative Health (R01AT007452, M.D.), the Burroughs Wellcome Fund (Investigator in the Pathogenesis of Infectious Disease Award, M.R.), and a predoctoral fellowship from the American Heart Association (S.K.). The funders had no role in study design, data collection and analysis, decision to publish or preparation of the manuscript. Obtaining human blood was supported by a Clinical Translational Science Award to the Institute for Clinical and Translation Science, UC Irvine.

References

1. Goronzy JJ & Weyand CM Mechanisms underlying T cell ageing. Nat Rev Immunol 19, 573–583, doi:10.1038/s41577-019-0180-1 (2019). [PubMed: 31186548]
2. Nikolich-Zugich J The twilight of immunity: emerging concepts in aging of the immune system. Nature immunology 19, 10–19, doi:10.1038/s41590-017-0006-x (2018). [PubMed: 29242543]
3. Centers for Disease, C. & Prevention. Estimates of deaths associated with seasonal influenza --- United States, 1976–2007. MMWR Morb Mortal Wkly Rep 59, 1057–1062 (2010). [PubMed: 20798667]
4. Wiersinga WJ, Rhodes A, Cheng AC, Peacock SJ & Prescott HC Pathophysiology, Transmission, Diagnosis, and Treatment of Coronavirus Disease 2019 (COVID-19): A Review. JAMA 324, 782–793, doi:10.1001/jama.2020.12839 (2020). [PubMed: 32648899]
5. Chen PL et al. Non-typhoidal Salmonella bacteraemia in elderly patients: an increased risk for endovascular infections, osteomyelitis and mortality. Epidemiol Infect 140, 2037–2044, doi:10.1017/S0950268811002901 (2012). [PubMed: 22261309]
6. Nichol KL, Nordin JD, Nelson DB, Mullooly JP & Hak E Effectiveness of influenza vaccine in the community-dwelling elderly. N Engl J Med 357, 1373–1381, doi:10.1056/NEJMoa070844 (2007). [PubMed: 17914038]
7. Targonski PV, Jacobson RM & Poland GA Immunosenescence: role and measurement in influenza vaccine response among the elderly. Vaccine 25, 3066–3069, doi:10.1016/j.vaccine.2007.01.025 (2007). [PubMed: 17275144]
8. Carrette F & Surh CD IL-7 signaling and CD127 receptor regulation in the control of T cell homeostasis. Semin Immunol 24, 209–217, doi:10.1016/j.smim.2012.04.010 (2012). [PubMed: 22551764]

9. den Braber I et al. Maintenance of peripheral naive T cells is sustained by thymus output in mice but not humans. Immunity 36, 288–297, doi:10.1016/j.immuni.2012.02.006 (2012). [PubMed: 22365666]
10. Qi Q et al. Diversity and clonal selection in the human T-cell repertoire. Proc Natl Acad Sci U S A 111, 13139–13144, doi:10.1073/pnas.1409155111 (2014). [PubMed: 25157137]
11. Li G et al. Decline in miR-181a expression with age impairs T cell receptor sensitivity by increasing DUSP6 activity. Nat Med 18, 1518–1524, doi:10.1038/nm.2963 (2012). [PubMed: 23023500]
12. Araujo L, Khim P, Mkhikian H, Mortales CL & Demetriou M Glycolysis and glutaminolysis cooperatively control T cell function by limiting metabolite supply to N-glycosylation. eLife 6, doi:10.7554/eLife.21330 (2017).
13. Chen IJ, Chen HL & Demetriou M Lateral compartmentalization of T cell receptor versus CD45 by galectin-N-glycan binding and microfilaments coordinate basal and activation signaling. J Biol Chem 282, 35361–35372, doi:10.1074/jbc.M706923200 (2007). [PubMed: 17897956]
14. Demetriou M, Granovsky M, Quaggin S & Dennis JW Negative regulation of T-cell activation and autoimmunity by Mgat5 N-glycosylation. Nature 409, 733–739, doi:10.1038/35055582 (2001). [PubMed: 11217864]
15. Dennis JW, Nabi IR & Demetriou M Metabolism, cell surface organization, and disease. Cell 139, 1229–1241, doi:10.1016/j.cell.2009.12.008 (2009). [PubMed: 20064370]
16. Lau KS et al. Complex N-glycan number and degree of branching cooperate to regulate cell proliferation and differentiation. Cell 129, 123–134, doi:10.1016/j.cell.2007.01.049 (2007). [PubMed: 17418791]
17. Mkhikian H et al. Genetics and the environment converge to dysregulate N-glycosylation in multiple sclerosis. Nat Commun 2, 334, doi:10.1038/ncomms1333 (2011). [PubMed: 21629267]
18. Mkhikian H et al. Golgi self-correction generates bioequivalent glycans to preserve cellular homeostasis. eLife 5, doi:10.7554/eLife.14814 (2016).
19. Mortales CL, Lee SU & Demetriou M N-Glycan Branching Is Required for Development of Mature B Cells. J Immunol 205, 630–636, doi:10.4049/jimmunol.2000101 (2020). [PubMed: 32591389]
20. Morgan R et al. N-acetylglucosaminyltransferase V (Mgat5)-mediated N-glycosylation negatively regulates Th1 cytokine production by T cells. J Immunol 173, 7200–7208, doi:10.4049/jimmunol.173.12.7200 (2004). [PubMed: 15585841]
21. Mortales CL, Lee SU, Manousadjian A, Hayama KL & Demetriou M N-Glycan Branching Decouples B Cell Innate and Adaptive Immunity to Control Inflammatory Demyelination. iScience 23, 101380, doi:10.1016/j.isci.2020.101380 (2020). [PubMed: 32745987]
22. Dennis JW, Warren CE, Granovsky M & Demetriou M Genetic defects in N-glycosylation and cellular diversity in mammals. Curr Opin Struct Biol 11, 601–607, doi:10.1016/s0959-440x(00)00254-2 (2001). [PubMed: 11785762]
23. Sy M et al. N-acetylglucosamine drives myelination by triggering oligodendrocyte precursor cell differentiation. J Biol Chem 295, 17413–17424, doi:10.1074/jbc.RA120.015595 (2020). [PubMed: 33453988]
24. Grigorian A & Demetriou M Mgat5 deficiency in T cells and experimental autoimmune encephalomyelitis. ISRN Neurol 2011, 374314, doi:10.5402/2011/374314 (2011). [PubMed: 22389815]
25. Bahaie NS et al. N-Glycans differentially regulate eosinophil and neutrophil recruitment during allergic airway inflammation. J Biol Chem 286, 38231–38241, doi:10.1074/jbc.M111.279554 (2011). [PubMed: 21911487]
26. Li CF et al. Hypomorphic MGAT5 polymorphisms promote multiple sclerosis cooperatively with MGAT1 and interleukin-2 and 7 receptor variants. Journal of neuroimmunology, doi:10.1016/j.jneuroim.2012.12.008 (2013).
27. Zhou RW et al. N-glycosylation bidirectionally extends the boundaries of thymocyte positive selection by decoupling Lck from Ca(2)(+) signaling. Nature immunology 15, 1038–1045, doi:10.1038/ni.3007 (2014). [PubMed: 25263124]

28. Lee SU et al. Increasing cell permeability of N-acetylglucosamine via 6-acetylation enhances capacity to suppress T-helper 1 (TH1)/TH17 responses and autoimmunity. PLoS One 14, e0214253, doi:10.1371/journal.pone.0214253 (2019). [PubMed: 30913278]
29. Grigorian A et al. Control of T Cell-mediated autoimmunity by metabolite flux to N-glycan biosynthesis. J Biol Chem 282, 20027–20035, doi:10.1074/jbc.M701890200 (2007). [PubMed: 17488719]
30. Lee SU et al. N-glycan processing deficiency promotes spontaneous inflammatory demyelination and neurodegeneration. J Biol Chem 282, 33725–33734, doi:10.1074/jbc.M704839200 (2007). [PubMed: 17855338]
31. Park JH et al. Suppression of IL7Ralpha transcription by IL-7 and other prosurvival cytokines: a novel mechanism for maximizing IL-7-dependent T cell survival. Immunity 21, 289–302, doi:10.1016/j.immuni.2004.07.016 (2004). [PubMed: 15308108]
32. Becklund BR et al. The aged lymphoid tissue environment fails to support naive T cell homeostasis. Sci Rep 6, 30842, doi:10.1038/srep30842 (2016). [PubMed: 27480406]
33. Martin CE et al. IL-7/anti-IL-7 mAb complexes augment cytokine potency in mice through association with IgG-Fc and by competition with IL-7R. Blood 121, 4484–4492, doi:10.1182/blood-2012-08-449215 (2013). [PubMed: 23610371]
34. Grabstein KH et al. Inhibition of murine B and T lymphopoiesis in vivo by an anti-interleukin 7 monoclonal antibody. J Exp Med 178, 257–264, doi:10.1084/jem.178.1.257 (1993). [PubMed: 8315381]
35. Martin CE et al. Interleukin-7 Availability Is Maintained by a Hematopoietic Cytokine Sink Comprising Innate Lymphoid Cells and T Cells. Immunity 47, 171–182 e174, doi:10.1016/j.immuni.2017.07.005 (2017). [PubMed: 28723549]
36. Weitzmann MN, Roggia C, Toraldo G, Weitzmann L & Pacifici R Increased production of IL-7 uncouples bone formation from bone resorption during estrogen deficiency. J Clin Invest 110, 1643–1650, doi:10.1172/JCI15687 (2002). [PubMed: 12464669]
37. Grigorian A et al. N-acetylglucosamine inhibits T-helper 1 (Th1) / T-helper 17 (Th17) responses and treats experimental autoimmune encephalomyelitis. J Biol Chem, doi:10.1074/jbc.M111.277814 (2011).
38. Blaschitz C & Raffatellu M Th17 cytokines and the gut mucosal barrier. J Clin Immunol 30, 196–203, doi:10.1007/s10875-010-9368-7 (2010). [PubMed: 20127275]
39. Liu JZ, Pezeshki M & Raffatellu M Th17 cytokines and host-pathogen interactions at the mucosa: dichotomies of help and harm. Cytokine 48, 156–160, doi:10.1016/j.cyto.2009.07.005 (2009). [PubMed: 19665391]
40. Parry CM et al. A retrospective study of secondary bacteraemia in hospitalised adults with community acquired non-typhoidal Salmonella gastroenteritis. BMC Infect Dis 13, 107, doi:10.1186/1471-2334-13-107 (2013). [PubMed: 23446179]
41. Ren Z et al. Effect of age on susceptibility to Salmonella Typhimurium infection in C57BL/6 mice. J Med Microbiol 58, 1559–1567, doi:10.1099/jmm.0.013250-0 (2009). [PubMed: 19729455]
42. Raffatellu M et al. Simian immunodeficiency virus-induced mucosal interleukin-17 deficiency promotes Salmonella dissemination from the gut. Nat Med 14, 421–428, doi:10.1038/nm1743 (2008). [PubMed: 18376406]
43. Geddes K et al. Identification of an innate T helper type 17 response to intestinal bacterial pathogens. Nat Med 17, 837–844, doi:10.1038/nm.2391 (2011). [PubMed: 21666695]
44. Vranjkovic A, Crawley AM, Gee K, Kumar A & Angel JB IL-7 decreases IL-7 receptor alpha (CD127) expression and induces the shedding of CD127 by human CD8+ T cells. Int Immunol 19, 1329–1339, doi:10.1093/intimm/dxm102 (2007). [PubMed: 17956896]
45. Sportes C et al. Administration of rhIL-7 in humans increases in vivo TCR repertoire diversity by preferential expansion of naive T cell subsets. J Exp Med 205, 1701–1714, doi:10.1084/jem.20071681 (2008). [PubMed: 18573906]
46. Kim HR, Hong MS, Dan JM & Kang I Altered IL-7Ralpha expression with aging and the potential implications of IL-7 therapy on CD8+ T-cell immune responses. Blood 107, 2855–2862, doi:10.1182/blood-2005-09-3560 (2006). [PubMed: 16357322]

47. Ucar D et al. The chromatin accessibility signature of human immune aging stems from CD8(+) T cells. J Exp Med 214, 3123–3144, doi:10.1084/jem.20170416 (2017). [PubMed: 28904110]

48. Abdel Rahman AM, Ryczko M, Pawling J & Dennis JW Probing the hexosamine biosynthetic pathway in human tumor cells by multitargeted tandem mass spectrometry. ACS Chem Biol 8, 2053–2062, doi:10.1021/cb4004173 (2013). [PubMed: 23875632]

49. Brandt AU et al. Association of a Marker of N-Acetylglucosamine With Progressive Multiple Sclerosis and Neurodegeneration. JAMA Neurol 78, 842–852, doi:10.1001/jamaneurol.2021.1116 (2021). [PubMed: 33970182]

50. Passtoors WM et al. IL7R gene expression network associates with human healthy ageing. Immun Ageing 12, 21, doi:10.1186/s12979-015-0048-6 (2015). [PubMed: 26566388]

51. Davey DA Androgens in women before and after the menopause and post bilateral oophorectomy: clinical effects and indications for testosterone therapy. Womens Health (Lond) 8, 437–446, doi:10.2217/whe.12.27 (2012). [PubMed: 22757734]

52. Taylor J et al. Transcriptomic profiles of aging in naive and memory CD4(+) cells from mice. Immun Ageing 14, 15, doi:10.1186/s12979-017-0092-5 (2017). [PubMed: 28642803]

53. Gubbels Bupp MR, Potluri T, Fink AL & Klein SL The Confluence of Sex Hormones and Aging on Immunity. Front Immunol 9, 1269, doi:10.3389/fimmu.2018.01269 (2018). [PubMed: 29915601]

54. Peckham H et al. Male sex identified by global COVID-19 meta-analysis as a risk factor for death and ITU admission. Nat Commun 11, 6317, doi:10.1038/s41467-020-19741-6 (2020). [PubMed: 33298944]

55. Takahashi T et al. Sex differences in immune responses that underlie COVID-19 disease outcomes. Nature 588, 315–320, doi:10.1038/s41586-020-2700-3 (2020). [PubMed: 32846427]

56. Bove RM et al. Effect of gender on late-onset multiple sclerosis. Mult Scler 18, 1472–1479, doi:10.1177/1352458512438236 (2012). [PubMed: 22383227]

57. Klein SL & Flanagan KL Sex differences in immune responses. Nat Rev Immunol 16, 626–638, doi:10.1038/nri.2016.90 (2016). [PubMed: 27546235]

58. Fink AL & Klein SL Sex and Gender Impact Immune Responses to Vaccines Among the Elderly. Physiology (Bethesda) 30, 408–416, doi:10.1152/physiol.00035.2015 (2015). [PubMed: 26525340]

59. Goss PE, Reid CL, Bailey D & Dennis JW Phase IB clinical trial of the oligosaccharide processing inhibitor swainsonine in patients with advanced malignancies. Clin Cancer Res 3, 1077–1086 (1997). [PubMed: 9815786]

60. Grigorian A & Demetriou M Manipulating cell surface glycoproteins by targeting N-glycan-galectin interactions. Methods Enzymol 480, 245–266, doi:10.1016/S0076-6879(10)80012-6 (2010). [PubMed: 20816213]

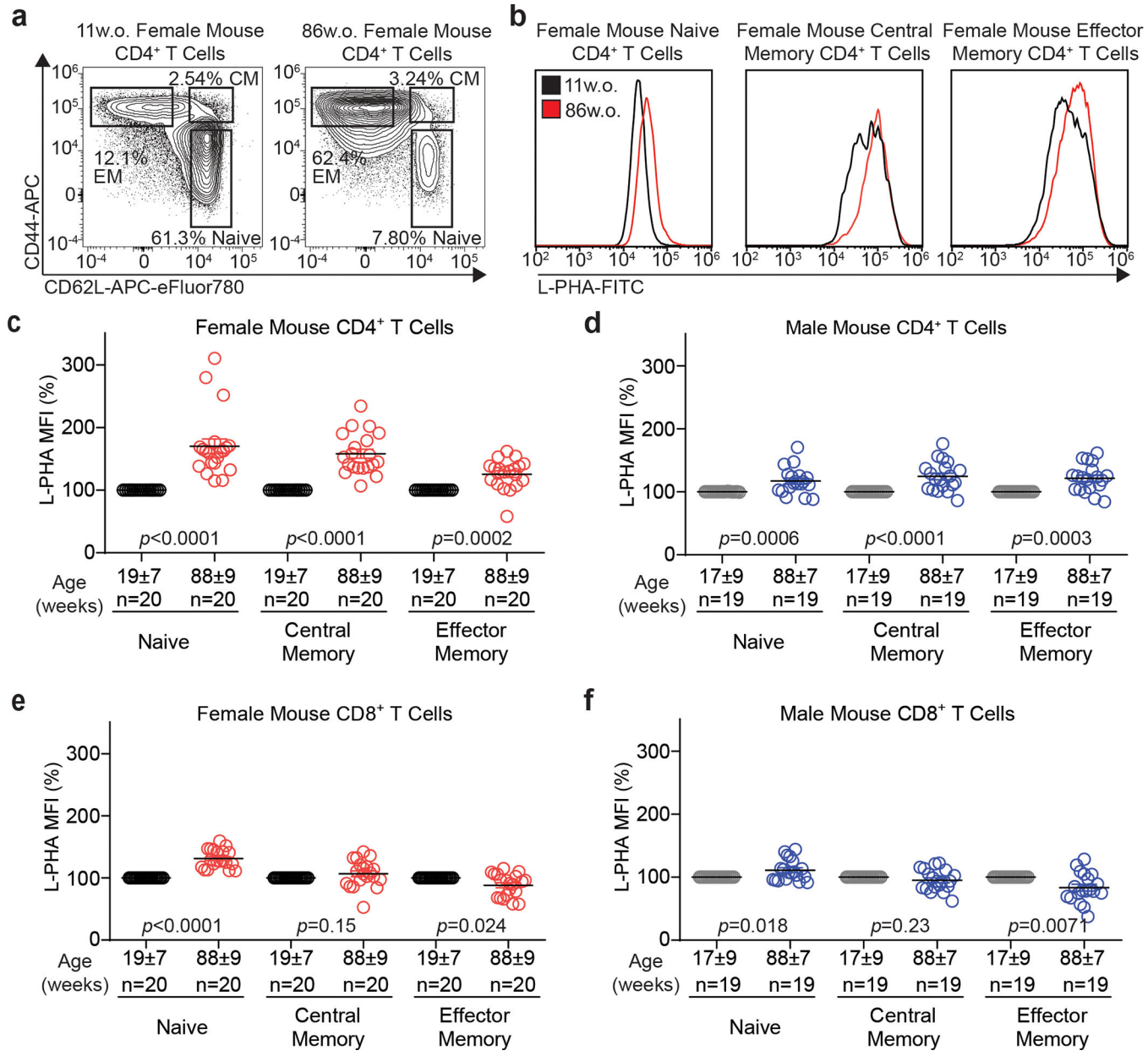

Figure 1. Mouse T cells display a sex-dimorphic increase in N-glycan branching with age.

a) Splenic T cells from representative young and old female mice were stained for naïve and memory markers, demonstrating naïve ($CD62L^+CD44^-$), central memory ($CD62L^+CD44^+$), and effector memory ($CD62L^-CD44^-$) subsets. **b)** L-PHA staining histograms of young and old female $CD4^+$ naïve, central memory, and effector memory T cell subsets. **c-f)** Splenic T cells from 20 young (range 7–32 weeks) and 20 old (range 74–113 weeks) female, as well as 19 young (range 7–31 weeks) and 19 old (range 80–100 weeks) male mice were analyzed in pairs by flow cytometry for L-PHA binding on naïve, central memory, or effector memory subsets. Analyses of female $CD4^+$ (**c**), male $CD4^+$ (**d**), female $CD8^+$ (**e**), and male $CD8^+$ (**f**) T cells are shown. Each symbol represents a single mouse. Each old mouse was normalized

to its young control. Age of mice in weeks with standard deviation is shown. P-values by two-tailed Wilcoxen test. Error bars indicate mean ± s.e.m.

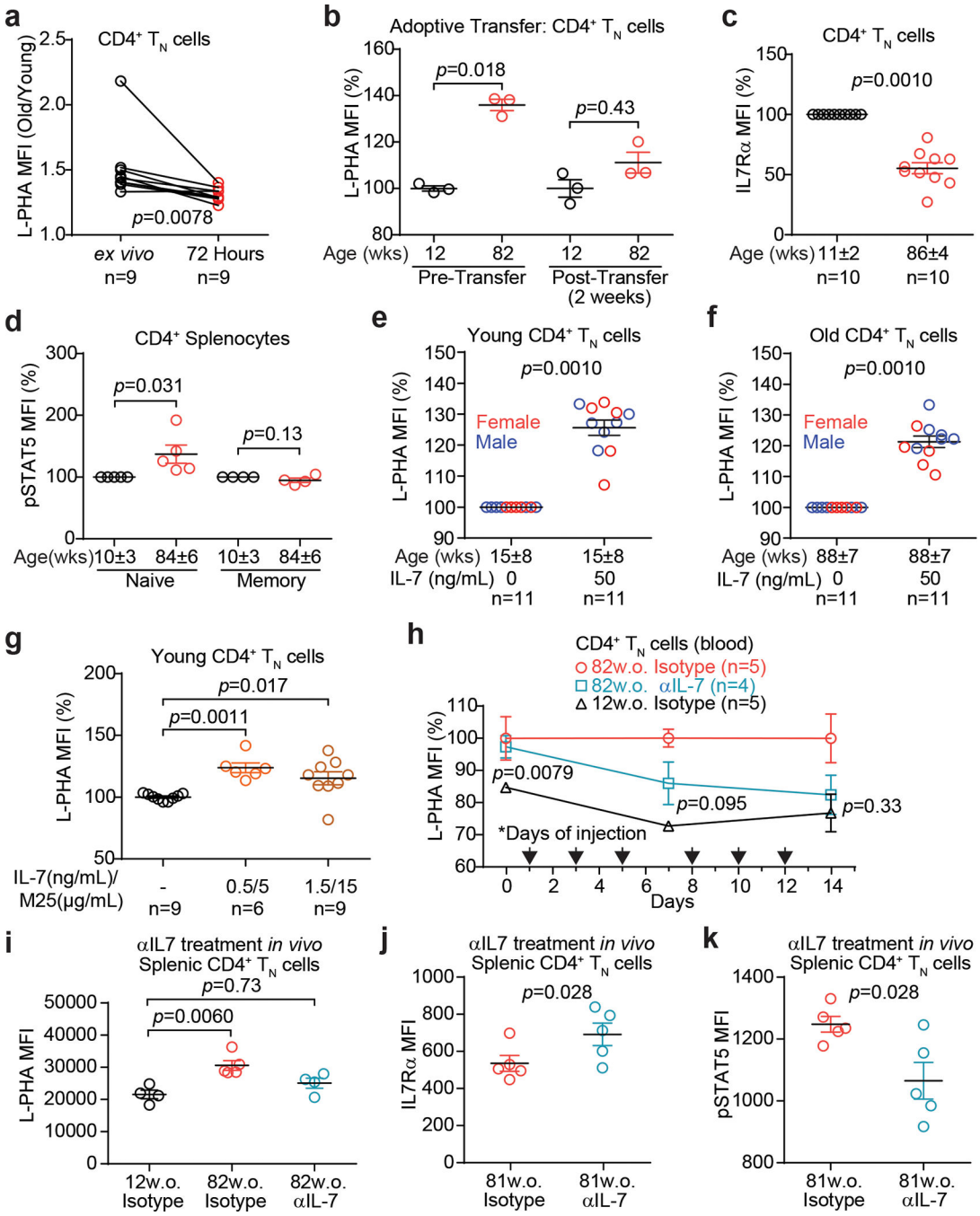

Figure 2. Elevated IL-7 signaling increases N-glycan branching in old female CD4$^+$ T$_N$ cells.

a) L-PHA flow cytometry of splenocytes gated on CD4$^+$ T$_N$ cells from young (12±4 weeks old) and old (86±3 weeks old) female mice immediately *ex vivo* and after 72 hours of rest in culture. Shown is L-PHA MFI ratio in old over young. **b)** Old and young female CD45.2$^+$ CD4$^+$ T$_N$ cells were adoptively transferred into young female CD45.1$^+$ recipient mice and analyzed by flow cytometry for L-PHA binding pre- and 2 weeks post-transfer, gating on CD4$^+$ T$_N$ cells. **c, d)** Flow cytometric analysis of IL7Rα (**c**) and pSTAT5 (**d**) in *ex vivo* naïve (**c, d**) and total memory (CD44$^+$) (**d**) CD4$^+$ T cells from young and old

female mice. **e, f)** Flow cytometric analysis of L-PHA binding on $CD4^+$ T_N cells from young (**e**) and old (**f**) female (red) and male (blue) mice treated with or without rhIL-7 (50ng/ml) in vitro for 72 hours. **g)** L-PHA flow cytometry gating on splenic $CD4^+$ T_N cells from young female mice following intraperitoneal injections of isotype control (1.5μg) or rhIL-7/M25 complex on days 1, 3, and 5. **h-k)** Flow cytometry gating on $CD4^+$ T_N cells from the blood (**h**) or spleen (**i-k**) of female mice following intraperitoneal injections of either isotype control (1.5mg) or anti-IL-7 antibody (M25, 1.5mg) 3 times a week for two (**h, i**) or four (**j, k**) weeks. Normalized geometric mean fluorescence intensity (MFI) is shown. Each symbol represents a single mouse. P-values determined by two-tailed Wilcoxon (**a, e, f**) Kruskal-Wallis with Dunn's multiple comparisons test (**b, g, i**), one-tailed Wilcoxon (**c, d**) or one-tailed Mann-Whitney (**h, j, k**). In panel (**h**) p-values indicate comparison of 12 w.o. isotype control group to 82 w.o. anti-IL7 treatment group. Error bars indicate mean ± s.e.m.

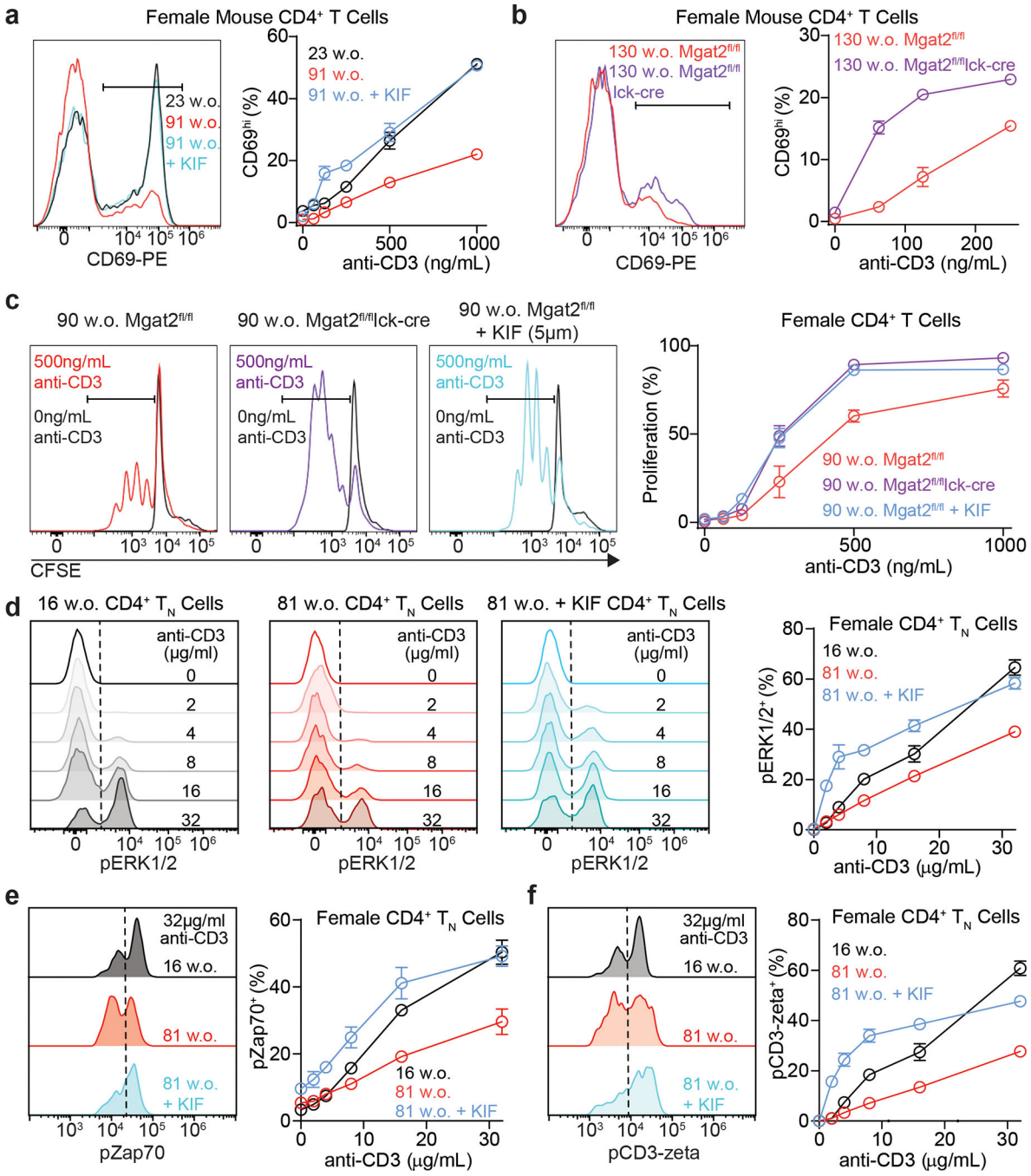

Figure 3. Age dependent increases in N-glycan branching suppress T cell function in female mice.

a-c) Splenocytes from female mice of the indicated ages and genotypes were activated with plate bound anti-CD3e for 24 (**a, b**) or 72 (**c**) hours in the presence or absence of 5μM kifunensine. Total CD4$^+$ T cells were analyzed for CD69 expression (**a, b**) or 5, 6-carboxyfluorescein diacetate succinimidyl ester (CFSE) dilution (**c**) by flow cytometry, gating additionally on L-PHA negative cells in *Mgat2$^{fl/fl}$/lck-cre* mice. **d-f)** Splenocytes from female mice of the indicated ages were pretreated with or without kifunensine for

24 hours, followed by activation with plate bound anti-CD3e for 15 minutes. Following fixation and permeabilization, phospho-ERK (**d**), phospho-Zap70 (**e**) or phospho-CD3zeta (**f**) induction was analyzed in $CD4^+$ T_N cells by flow cytometry. Data are representative of at least three independent experiments. Error bars indicate mean ± s.e.m.

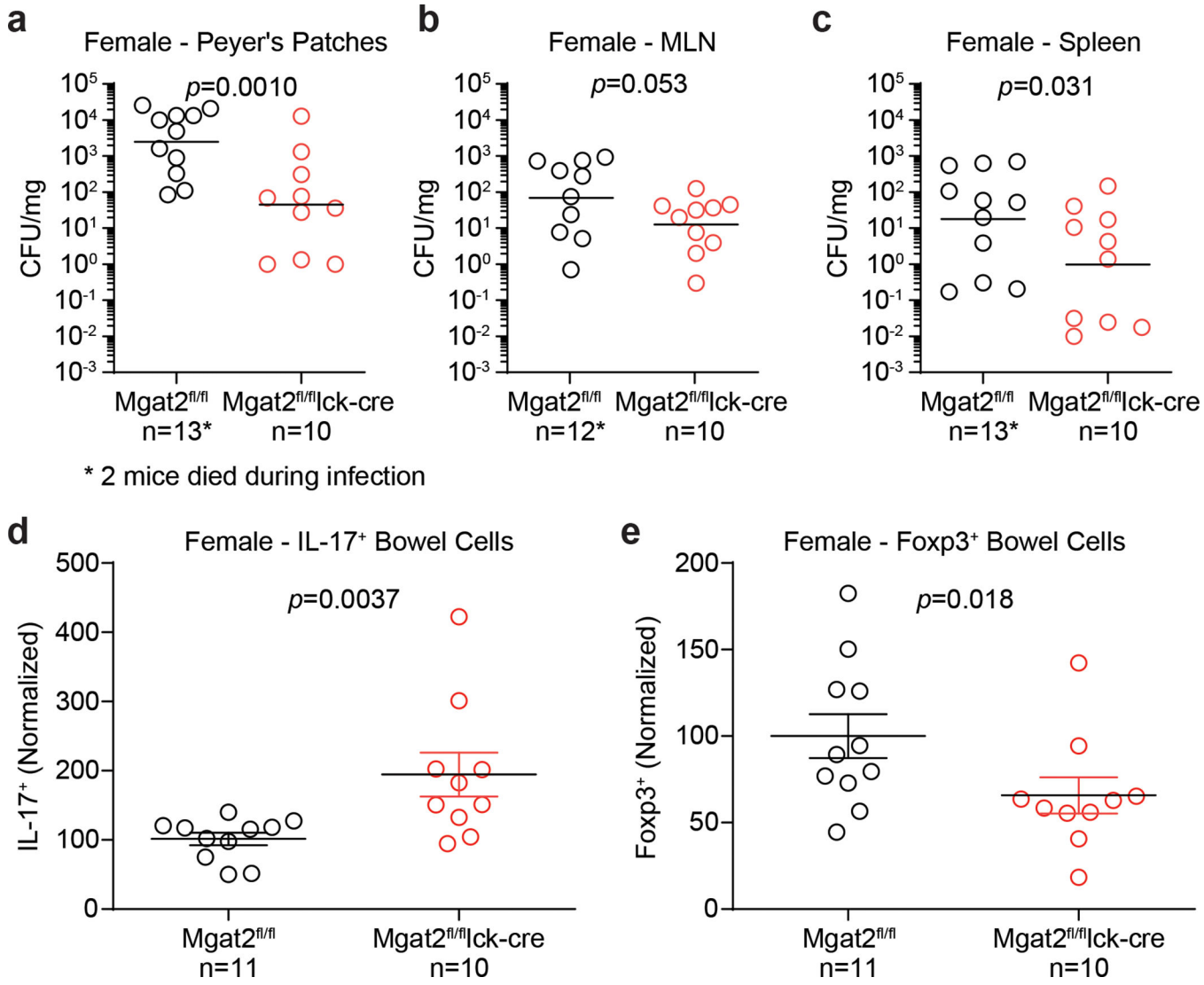

Figure 4. Elevated N-glycan branching in T cells suppresses immune response to Salmonella in old female mice.

a-e) *Mgat2*$^{fl/fl}$ and *Mgat2*$^{fl/fl}$*lck-cre* female mice were pre-treated with streptomycin intragastrically one day prior to inoculation with S. Typhimurium (5×10^8 colony forming units (CFU) per mouse). CFU in Peyer's patches (**a**), mesenteric lymph nodes (MLN; **b**), and spleen (**c**) were enumerated 72 hours after infection. Total IL-17$^+$ (**d**) and Foxp3$^+$ (**e**) cells within the gut were detected by flow cytometry and normalized to the average number of cells from *Mgat2*$^{fl/fl}$ mice. Each symbol represents a single mouse. P-values by one-tailed Mann-Whitney. Bars indicate geometric mean (**a-c**) or mean ± s.e.m (**d, e**).

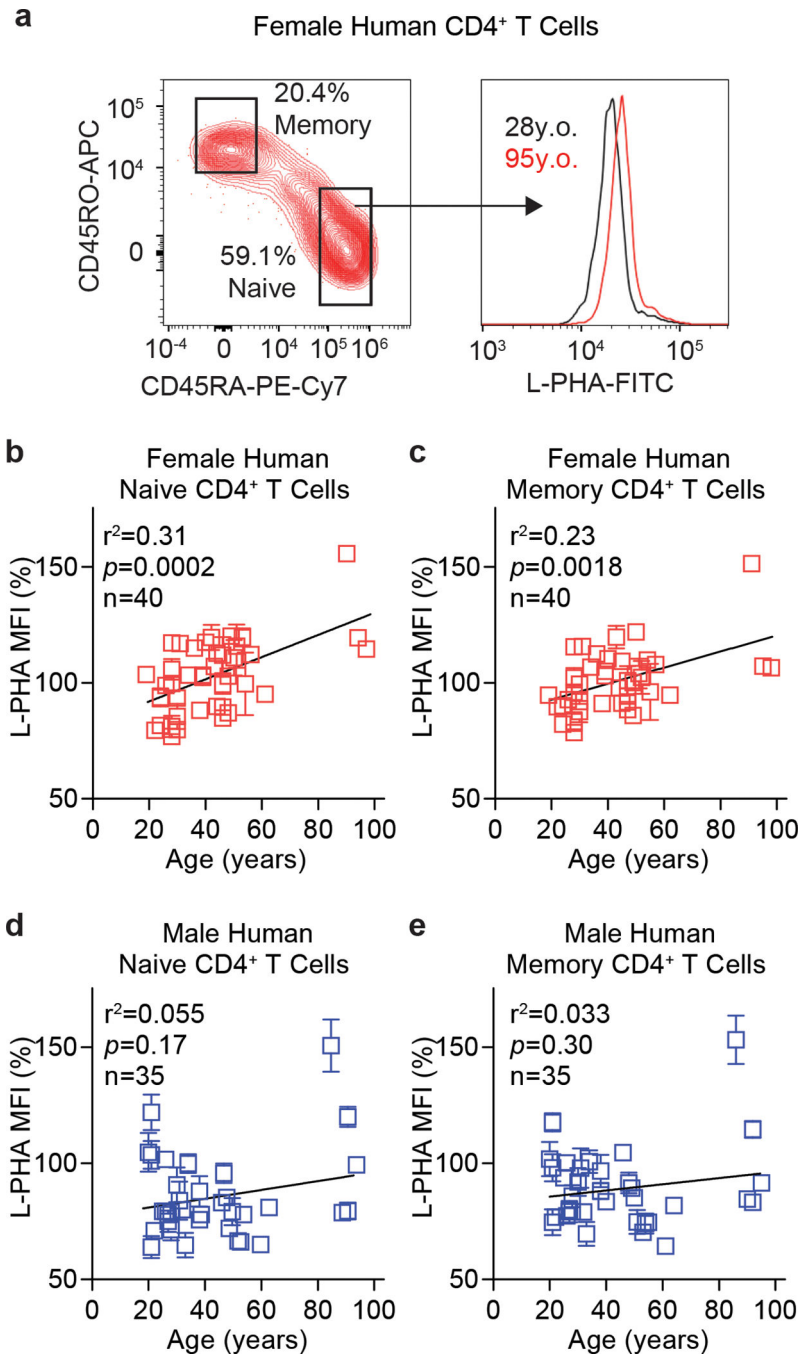

Figure 5. N-glycan branching increases with age in human T cells.

a-e) L-PHA flow cytometry of human PBMCs from healthy females (**a-c**) and males (**d, e**), gating on naïve $CD4^+$ ($CD45RA^+$ $CD45RO^-$; **b, d**) or memory $CD4^+$ ($CD45RA^-CD45RO^+$; **c, e**) T cells. Data were normalized to a reference control across experiments. Each symbol represents a single individual. R^2 and p-values by linear regression. Error bars indicate mean ± s.e.m.

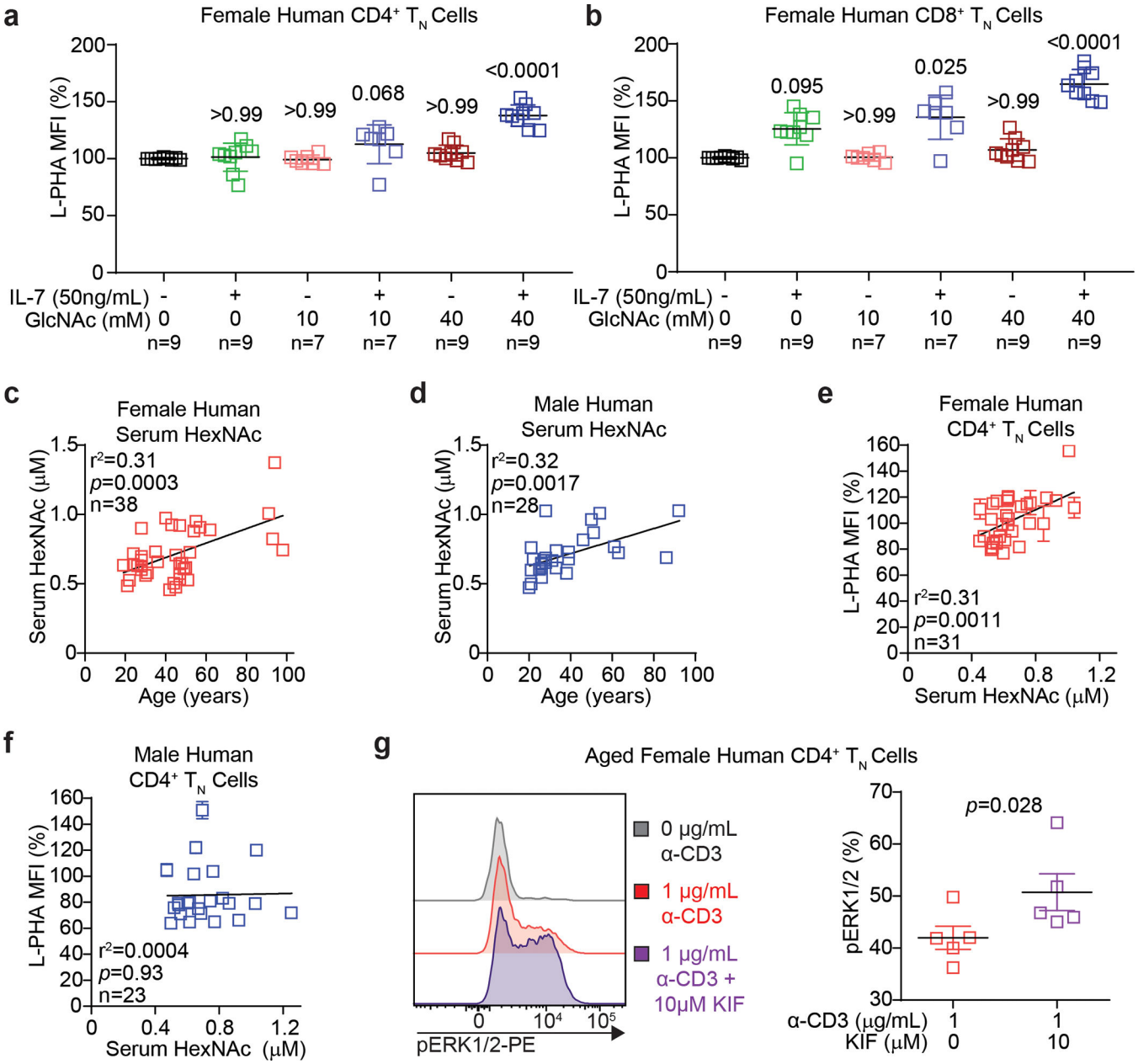

Figure 6. Serum N-acetylglucosamine increases with age and synergizes with IL-7 to raise N-glycan branching in human T cells.

a, b) PBMCs from healthy female donors (28–45 years old) were cultured with or without rhIL-7 (50ng/ml) and/or GlcNAc (10mM or 40mM) for 9 days, then analyzed for L-PHA binding by flow cytometry, gating on $CD4^+$ T_N cells (**a**) or $CD8^+$ T_N cells (**b**). **c, d)** Human serum from healthy female (**c**; 19–98 years old; 45±20 years old) or male (**d**; 20–92 years old; 38±19 years old) donors of the indicated ages was analyzed for HexNAc levels by LC-MS/MS. **e, f)** Correlation of serum HexNAc with L-PHA binding on $CD4^+$ T_N cells in healthy female (**e**; 19–98 years old; 44±20 years old) or male (**f**; 20–92 years old; 40±20 years old) donors. **g)** Flow cytometric analysis of intracellular pERK1/2 in 90–94 year old female human $CD4^+$ T_N cells stimulated with plate bound anti-CD3 for 15 minutes. Cells

were pre-treated with or without 10μM kifunensine for 24 hours prior to stimulation. Each symbol represents a single individual. Normalized geometric mean fluorescence intensity (MFI) is shown (**a, b, e, f**). P-values by Kruskal-Wallis with Dunn's multiple comparisons test (**a,b**), linear regression (**c-f**), and one-tailed Mann-Whitney (**g**). Error bars indicate mean ± s.e.m.

Table 1.

Differential expression of IL-7 signaling-pathway genes in aging

		Naïve				Memory			
		Female		Male		Female		Male	
Gene Symbol	**Gene Description**	**Adj p Value**	**Fold Change**	**Adj p Value**	**Fold Change**	**Adj p Value**	**Fold Change**	**Adj p Value**	**Fold Change**
Il7r	Interleukin 7 receptor alpha	1.80E-02	0.6273	7.42E-01	0.8618	9.52E-01	0.9778	1.51E-01	0.6728
Jak3	Janus kinase 3	6.67E-15	2.6892	1.20E-01	1.4740	2.40E-01	1.3606	3.41E-01	1.2346
Socs1	Suppressor of cytokine signaling 1	1.81E-08	2.6417	9.99E-01	1.0142	1.49E-03	1.9095	5.85E-01	−0.3558
Socs3	Suppressor of cytokine signaling 3	4.49E-21	5.9106	6.84E-01	1.8401	1.78E-20	6.3359	2.62E-08	2.9469
Jak1	Janus kinase 1	6.62E-01	0.7575	9.77E-01	1.0459	1.64E-01	0.6826	6.21E-01	0.7994
Il2rg	Interleukin 2 receptor, gamma chain	7.52E-01	1.1804	9.49E-01	1.0542	8.70E-01	1.0482	7.11E-01	0.8967
Stat5a	Signal transducer and activator of transcription 5A	6.36E-01	1.2806	9.27E-01	1.1085	8.72E-01	1.0665	9.35E-01	1.0502